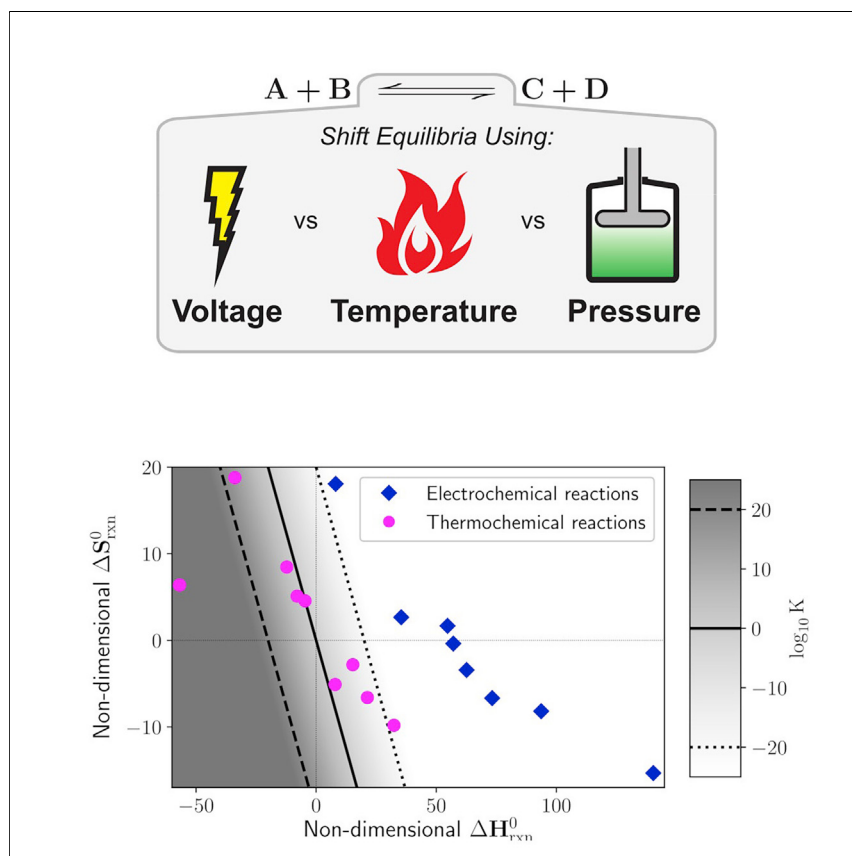


Article

Thermodynamic Discrimination between Energy Sources for Chemical Reactions



In this work, we develop a framework to compare thermodynamic driving forces, namely temperature (thermal energy), pressure (mechanical energy), and voltage (electrical energy). When applied to multiple industrially practiced and next-generation reactions, our analysis reveals a clear division between reactions that traditionally rely on pressure and temperature as energy sources and those that rely on voltage. Our formulation provides a universal framework through which the impact of diverse energy sources on chemical equilibria can be compared and understood.

Zachary J. Schiffer, Aditya M.

Limaye, Karthish Manthiram

karthish@mit.edu

HIGHLIGHTS

Reaction-independent, non-dimensional expression for chemical equilibrium is developed

Temperature, pressure, and voltage are compared as driving forces for chemical synthesis

Visualization reveals divide between electro- and thermochemical reactions



Article

Thermodynamic Discrimination between Energy Sources for Chemical Reactions

Zachary J. Schiffer,¹ Aditya M. Limaye,¹ and Karthish Manthiram^{1,2,*}

SUMMARY

Chemical transformations traverse large energy differences, yet the comparison of energy sources to drive a reaction is often done on a case-by-case basis; there is no fundamentally driven, universal framework with which to analyze and compare driving forces for chemical reactions. In this work, we present a reaction-independent expression for the equilibrium constant as a function of temperature, pressure, and voltage. With a specific set of axes, all reactions are represented by a single (x, y) point, and a quantitative divide between electrochemically and thermochemically driven reactions is visually evident. Additionally, we show that our expression has a strong physical basis in work and energy fluxes to the system, although specific data about operating conditions are necessary to provide a quantitative energy analysis. Overall, this universal equation and facile visualization of chemical reactions provides a consistent thermodynamic framework for comparing electrochemical versus thermochemical energy sources without knowledge of detailed process parameters.

INTRODUCTION

In chemical synthesis, the making and breaking of chemical bonds often requires traversing large energy differences. In fact, the basic chemical industry accounts for close to 20% of total delivered energy consumption in the industrial sector, which itself uses the most delivered energy of any end-use sector globally (54%).^{1,2} Traditionally, industrial chemical synthesis has relied on pressure and temperature as driving forces to synthesize chemicals; a reactor requires an exchange of heat and work in order to drive a chemical transformation.^{2–4} Yet, with the advent of abundant and accessible renewable electricity, it is attractive to consider driving chemical reactions that are conventionally driven with temperature and pressure with electrical voltage instead.^{5–9} Hence, one is confronted with the question, “why should a given chemical reaction be driven preferentially with temperature (thermal energy), pressure (mechanical energy), or voltage (electrical energy)?” The response to this question is generally either broad and qualitative or extremely reaction specific. Broadly, if a reaction is highly endothermic (results in a very positive change in enthalpy), then one may prefer an electrochemical approach that avoids excessively high operating temperatures to shift the equilibrium toward products.^{9,10} Additionally, if a reaction requires high pressures to drive conversion to products via Le Chatelier’s principle, then one may prefer using voltage to avoid these excessively high pressures. Technoeconomic analyses are also often used to discriminate between thermochemical and electrochemical driving forces based on feedstock costs and system efficiencies.^{11–16} However, these technoeconomic analyses remain focused on specific reactions without investigating the physical basis for the preference of driving force in a general manner. While many of the choices in the driving forces for chemical reactions are determined by factors such as kinetics, cost, and safety, research and development often begins before estimates of these specific parameters

Context & Scale

The equilibrium of a chemical reaction can be shifted using various driving forces, including temperature (thermal energy), pressure (mechanical energy), and voltage (electrical energy). These driving forces are often compared with technoeconomic analyses that discriminate between mature chemical synthesis routes where associated costs can be tabulated. Here, we demonstrate how thermodynamic analyses provide a framework to compare and discriminate between energy sources for chemical reactions. This methodology is useful for comparisons of less developed synthetic routes where accurate costs cannot be ascribed. Specifically, our analysis provides a universal, non-dimensional framework through which the effect of temperature, pressure, and voltage on reactions can be understood. This is articulated in both the context of chemical equilibria and energy exchanges, providing understanding across industrially practiced and next-generation chemical synthesis routes.



are known. Accordingly, an intermediate-level framework for comparing driving forces based on available physical parameters is missing; specifically, one that is simple and intuitive, yet also quantitative and dependable across a wide range of chemical reactions.

We address the question of how to compare and discriminate between energy sources for driving chemical reactions via a theoretical framework built around reaction thermodynamics. Efficiency and thermodynamic limits on extraction of useful work have been studied for centuries (e.g., with the Carnot engine),^{17,18} and more recent work has slowly relaxed ideal constraints to add in real-world practicalities via developments in fields such as endoreversible thermodynamics and finite-time thermodynamics.^{19,20} However, these theories are often built to describe the extraction of energy from a chemical reaction, e.g., in a combustion engine, and they often still require significant knowledge of specific process parameters such as heat transfer coefficients, compressor efficiencies, thermodynamic paths, etc.²¹ In this work, we construct a universal equation to describe and analyze the thermodynamics of chemical reactions driven by temperature, pressure, and voltage. We have focused on these driving forces due to their prevalence in chemical synthesis, although the analysis can be extended to the direct use of photons or mechanochemical methods. We compare heat, mechanical work, and electrical work as energy inputs to a chemical system and find that an ideal, lossless model of energy comparison provides a physical basis for our non-dimensional thermodynamic parameter analysis. After constructing a universal equation, we then introduce a facile visualization method for comparing chemical reactions, with a focus on redox reactions (voltage is generally not an option for non-redox reactions) and show a clear divide between chemical reactions traditionally driven by elevated temperatures and pressures in industry and reactions that rely on electrical voltage. Our approach provides a simple, universal framework with a thermodynamic basis to compare and justify using temperature, pressure, or voltage as a driving force for a chemical reaction, and our analysis can be leveraged by researchers in a broad range of fields to help determine the important systems-level choice of thermodynamic driving force.

RESULTS AND DISCUSSION

Non-dimensionalization of Reaction Equilibrium

We are interested in comparing the effects of temperature, pressure, and voltage as driving forces for shifting the equilibrium of a chemical reaction. Accordingly, we start with a chemical reaction that has some defined stoichiometry given by:

$$\sum_i \nu_i A_i = 0, \quad (\text{Equation 1})$$

where ν_i are the stoichiometric coefficients for chemical species A_i . Chemical equilibrium at constant temperature (T), pressure (P), and voltage (E) provides the constraint:

$$\sum_i \nu_i \mu_i(T, P, E) = 0, \quad (\text{Equation 2})$$

where μ_i are the species electrochemical potentials. Assuming that the system is an ideal mixture of gases and that $\Delta C_{P,\text{rxn}} \equiv \sum \nu_i C_{P,i} = 0$, the equilibrium constant, K , is a simple function of thermodynamic variables (Derivation S1)^{22–24}:

$$\begin{aligned} \log_e K &= \frac{-\Delta G_{\text{rxn}}(T, P, E)}{RT} \\ &= -\frac{\Delta H_{\text{rxn}}^0}{RT} - \frac{n_{e^-} FE}{RT} - \Delta n_{\text{rxn}} \log_e \frac{P}{P^0} + \frac{\Delta S_{\text{rxn}}^0}{R}, \end{aligned} \quad (\text{Equation 3})$$

¹Department of Chemical Engineering,
Massachusetts Institute of Technology,
Cambridge, MA 02139, USA

²Lead Contact

*Correspondence: karthish@mit.edu

<https://doi.org/10.1016/j.joule.2020.12.014>

where ΔH_{rxn}^0 and ΔS_{rxn}^0 are the enthalpy and entropy of reaction, respectively, at ambient conditions (namely no applied voltage, $T = T^0 = 298.15\text{ K}$, and $P = P^0 = 1\text{ bar}$), R is the ideal gas constant, n_{e^-} is the minimum number of electrons necessarily transferred in the overall reaction ([Derivation S1](#)), and $\Delta n_{rxn} \equiv \sum_{i \in \text{gas}} \nu_i$.

Although we assume for simplicity that all of our components are gases (with a few exceptions for pure liquids and solids), the extension to liquids, dissolved species, and solids is not difficult to incorporate when going through the full derivation ([Derivation S1](#)). [Equation 3](#) is a familiar description of the equilibrium constant with one major difference: we have defined $K \equiv \prod_{i \in \text{gas}} y_i^{\nu_i}$, with y_i being the mole fraction of each component in the gas phase, instead of the more traditional $K = \prod_i p_i^{\nu_i}$, where p_i is the partial pressure of a species (i.e., the activity of an ideal gas).²⁵ In this work, the equilibrium constant is defined by [Equation 3](#) instead of the traditional definition so that pressure will be explicitly included in the expression. Through [Equation 3](#) and proper stoichiometry normalization, we can better compare reaction equilibria based on a more consistent relationship between mole fractions and K that is not present when K is written in terms of activity (e.g., partial pressures) instead of mole fractions.

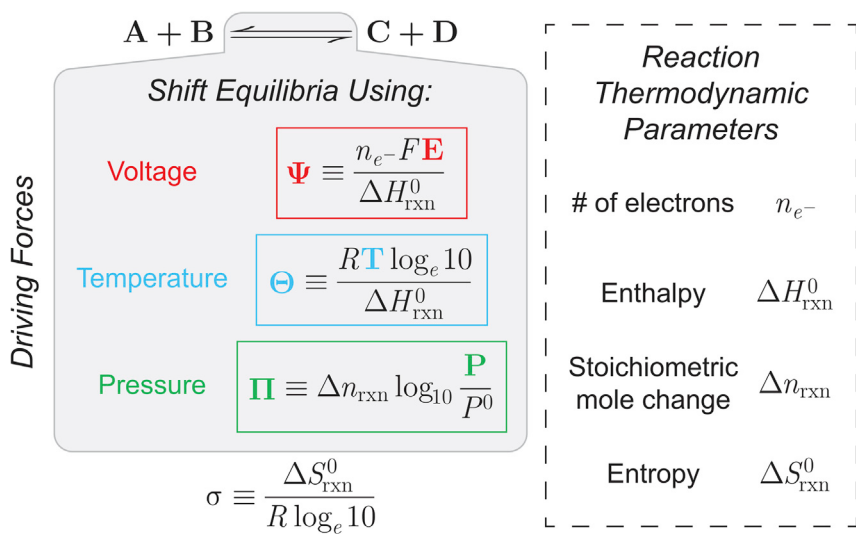
The practically relevant quantity for describing a chemical reaction is conversion, not the equilibrium constant. However, conversion will be dependent on the exact reaction equation and not a universal function. To keep the analysis general, the equilibrium constant, K , will be used as a proxy for conversion since conversion is a strictly increasing, sigmoidal function of K ranging from 0 to 1 ([Derivation S2](#)).

Unfortunately, the expression for the equilibrium constant given by [Equation 3](#) does not allow for facile comparison of temperature, pressure, and voltage in its current form since the quantities ΔH_{rxn}^0 , ΔS_{rxn}^0 , Δn_{rxn} , and n_{e^-} are reaction-specific, preventing a general analysis of chemical reaction equilibrium. To facilitate a comparison, the equilibrium constant expression can be non-dimensionalized to remove any specifics about the chemical reaction. Non-dimensionalization is a useful tool for solving differential equations in certain limits and for quickly determining characteristic properties of a system such as time and length; for these reasons it finds wide use across the fields of chemical engineering, physics, fluid dynamics, etc.²⁶ In the case of a chemical reaction, non-dimensionalization combines the reaction-specific details of the system with the reaction operating conditions to create new variables that are reaction-independent and scale simply with the thermodynamic driving forces of interest ([Figure 1](#); [Derivation S3](#)). Traditional non-dimensionalization, e.g., of reaction-diffusion systems, relies on the structure of a differential equation to provide the non-dimensional groupings; an algebraic equation such as [Equation 3](#) does not have equivalently straightforward non-dimensional groupings, and non-dimensionalization must instead rely on underlying physical intuition.

[Equation 3](#) can be non-dimensionalized to achieve a universal expression for how thermal, mechanical, and electrical energy shift the chemical equilibrium through non-dimensional temperature ($T \rightarrow \Theta$), pressure ($P \rightarrow \Pi$), and voltage ($E \rightarrow \Psi$):

$$\Theta \equiv \frac{RT \log_e 10}{\Delta H_{rxn}^0},$$

$$\Pi \equiv \Delta n_{rxn} \log_{10} \frac{P}{P^0},$$

**Figure 1. Non-dimensionalization Scheme for Thermodynamic Variables**

Given a generic reaction, here shown as the conversion of reactants A and B to products C and D, reaction-specific thermodynamic parameters (right) and the reaction operation conditions (left) can be combined to obtain non-dimensional groupings that scale with the thermodynamic driving forces and enable non-dimensionalization of [Equation 3](#) to obtain [Equation 4](#).

$$\Psi \equiv \frac{n_{e^-} F E}{\Delta H_{rxn}^0},$$

$$\sigma \equiv \frac{\Delta S_{rxn}}{R \log_e 10},$$

$$\log_{10} K = -\frac{1}{\Theta} - \frac{\Psi}{\Theta} - \Pi + \sigma. \quad (\text{Equation 4})$$

Note that we have chosen to use $\Theta \propto T$ instead of a potentially "natural" quantity $\Theta \propto 1/T$ so that changes in Θ are more intuitively interpretable.²⁷ One of the advantages of [Equation 4](#) is that all reactions collapse onto simple plots that show the equilibrium constant, a proxy for reaction conversion, as a function of non-dimensional thermodynamic driving forces ([Figure 2](#)). This visualization reveals that crossing equilibrium contours with pressure requires a larger relative increase in thermodynamic driving force than crossing equilibrium contours with temperature or voltage (further supporting analysis of contours and derivatives provided in [Derivation S4](#)). This discrepancy is magnified by the fact that the scaling of Π is logarithmic with pressure whereas the scalings of Θ and Ψ are linear with temperature and voltage, respectively.

So far, the analysis has relied on the mathematical form of our non-dimensional parameters. In practice, there are many alternative non-dimensional groupings with additional constant factors or functional forms that would change this analysis. However, these non-dimensional thermodynamic parameters ([Figure 1](#)) are not only convenient from a mathematical perspective but also represent physical groupings related to analogous work and energy fluxes, discussed below, such that conclusions drawn from analysis of the non-dimensional thermodynamic parameters are physically relevant.

Work and Energy Exchange

A direct comparison between temperature, pressure, and voltage is difficult since each driving force has different units. Even with our non-dimensional scalings, there

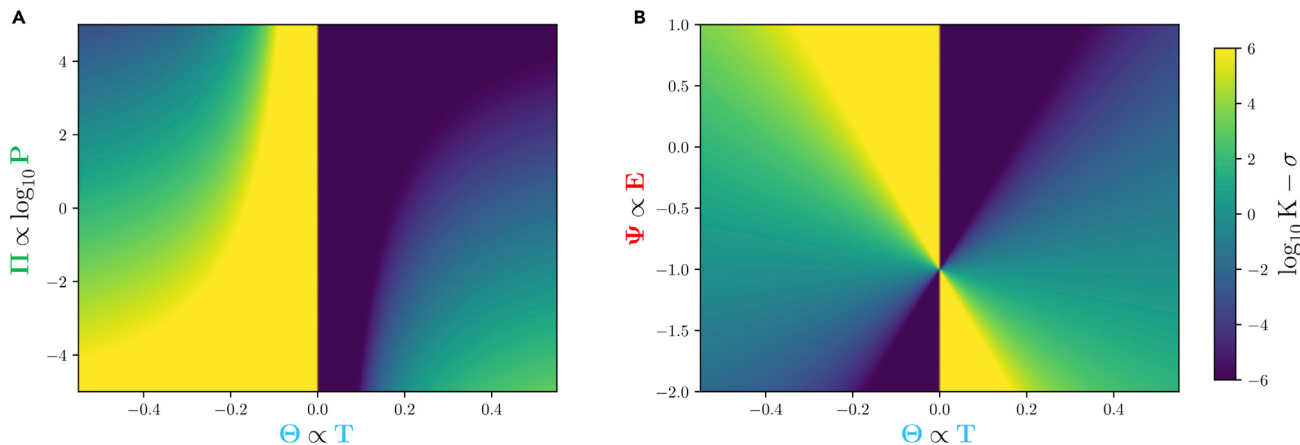


Figure 2. Plots of Equation 4

(A and B) Every chemical reaction can be mapped onto these universal plots. When no voltage is applied ($\Psi = 0$), contours showing how pressure and temperature affect reaction equilibrium are visualized (A). At ambient pressure ($\Pi = 0$), contours showing how voltage and temperature affect the reaction equilibrium are visualized (B). Contours of how voltage and pressure affect the equilibrium at 298.15 K (ambient temperature) are not as simple to visualize; there is a Θ^{ambient} term in these contours that make the plot less useful because it is reaction dependent and not generalizable (these plots and full discussion in [Derivation S4](#)). Crossing the constant K contours using pressure requires a larger relative change in non-dimensional driving force than it does using voltage or temperature. Note that the colorbar axis is $\log_{10} K - \sigma$ so that the plot remains independent of reaction; different reactions will essentially provide a constant shift from σ that does not change the shape of the plot. Additionally, crossing $\Theta = 0$ for a given reaction is impossible since the sign of Θ is determined by the reaction enthalpy (a fixed quantity assuming $\Delta C_{P,\text{rxn}} = 0$).

is no reason to assume *a priori* that these non-dimensional parameters have any physical meaning and can be directly compared with each other. Instead, a metric for comparing driving forces on equal footing would be to compare work and energy exchanges of the system; this comparison will provide a physical basis for our non-dimensional parameters so that we can directly compare them.

In practice, no general method to convert between thermodynamic parameters and work exists since heat and work are path functions. However, if the system does not have any energy losses, the overall, steady-state energy exchanges of the system must obey the law of energy conservation:

$$W_M + W_E + Q = \Delta H_{\text{rxn}}^0 \cdot z, \quad (\text{Equation 5})$$

where z is the reaction conversion at equilibrium, a function of K and defined between 0 and 1. A more convenient form of [Equation 5](#) results from non-dimensionalization of the work terms with the reaction enthalpy as the characteristic energy of the system ([Derivation S5](#)):

$$\Omega_{W_M} + \Omega_{W_E} + \Omega_Q = z. \quad (\text{Equation 6})$$

Ignoring the exact functional form of the work terms for now and assuming that the system is driven by either pressure or voltage individually, but not both simultaneously, the constraint imposed by [Equation 6](#) has the geometric form of a plane in Ω_W - Ω_Q space ([Figure 3](#)). Accordingly, for a system with no energy losses, any energy input will result in an equivalent change in conversion, regardless of the energy source. If additional information is available, such as the cost of electricity, efficiency of heat flux, compressor losses, etc., there are a multitude of thermodynamic and technoeconomic heuristics that can lead to a quantitative conclusion, but these are beyond the scope of this work.

In the absence of more information, there are still important insights to glean from the functional forms of the work and heat inputs. In addition to the previous

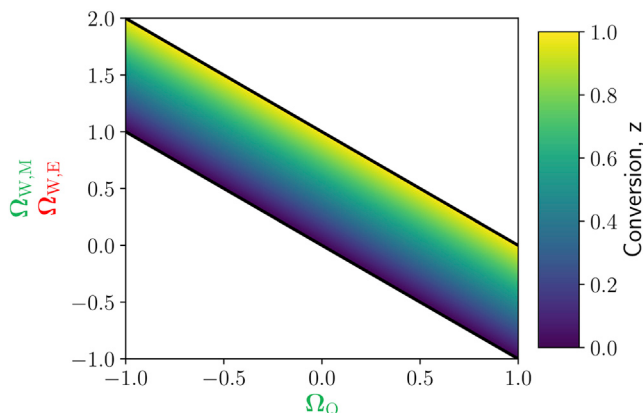


Figure 3. Conversion, z , as a Function of Various Energy Inputs Assuming No Energy Losses in the System

In this system, either pressure or voltage is utilized, but not both simultaneously. In the absence of losses, all energy exchanges produce the same change in conversion, regardless of the source of the energy. Thus, in the absence of additional, reaction- and process-specific information, this energy analysis simply provides a physical basis for the non-dimensional analysis, as discussed in the main text.

assumptions (ideal gas mixture and $\Delta C_{P,\text{rxn}} = 0$), additional assumptions are necessary to convert from thermodynamic parameters to work and energy fluxes: (1) the reactor is isothermal, isobaric, and does not exchange mechanical work with the environment, and (2) the processes that bring the inputs to the operating conditions and bring the outputs back to ambient conditions have access to a single heat bath at some T_{bath} . Given these assumptions, as well as assuming unit efficiency of every process, the total energy and work exchanges with the overall system are functions of the previous thermodynamic parameters, the conversion, $z = z(K)$, which is a function of the equilibrium constant, and the single non-dimensional thermal bath temperature, $\Theta_{\text{bath}} \equiv \frac{RT_{\text{bath}} \log_e 10}{\Delta H_{\text{rxn}}^0}$, that is used to bring reactants to operating conditions and products to ambient conditions ([Derivation S5](#))^{28–31}:

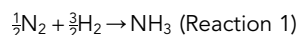
$$\begin{aligned}\Omega_{W_E} &= -z(K)\Psi \\ \Omega_{W_M} &= -z(K)\Theta_{\text{bath}}\Pi \\ \Omega_Q &= z(K)(\Psi + \Theta_{\text{bath}}\Pi + 1)\end{aligned}\quad (\text{Equation 7})$$

Without additional practical information, our energy analysis is qualitative, and these equations by themselves do not reveal a preference for mechanical work, electrical work, or heat. However, these equations do provide justification for our previous analysis. We initially began our reaction analysis by non-dimensionalizing temperature, pressure, and voltage to remove any reaction-specific quantities from the equilibrium expression given in [Equation 3](#). The chosen non-dimensionalizations are intuitive; although these parameter groupings are relatively common throughout the literature (e.g., Π is found in the Nernst equation and Ψ is related to the thermo-neutral voltage), the physical basis of these non-dimensional parameters (Θ , Π , and Ψ) on an energy basis has not been described. The energy analysis presented here, however, reveals that the non-dimensional electrical work (Ω_{W_E}) will scale directly with non-dimensional voltage (Ψ), the non-dimensional mechanical work (Ω_{W_M}) will scale directly with non-dimensional pressure (Π), and the heat flux is a convolution of all the energy inputs but has a clear characteristic energy given by ΔH_{rxn}^0 , which was used to non-dimensionalize temperature (Θ). Accordingly, although the previous analysis dealt with non-dimensional driving forces that were not, *a priori*, comparable, this energy analysis reveals that these non-dimensional

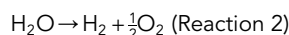
quantities are reasonable proxies for work and energy exchanges and that our non-dimensional analysis has a strong physical basis. Direct comparisons of the non-dimensional thermodynamic parameters therefore correspond to comparisons of analogous energy and work exchanges, validating conclusions drawn from such direct comparisons.

Example Chemical Reactions on Universal Plot

While the universal colormaps of [Equation 4](#) are interesting on their own ([Figure 2](#)), contour lines of constant K for a specific reaction help visualize the thermodynamics of that reaction. This is the advantage of plotting the equilibrium constant in non-dimensional space: instead of qualitatively looking at endo- versus exothermicity or analyzing a specific reaction's equilibrium constant at various temperatures, pressures, and voltages, we can quantitatively display the influence of these driving forces on a single set of axes since the thermodynamic landscapes for individual reactions all collapse onto a single plot in non-dimensional space ([Figure 2](#)). Two well-studied reactions are ammonia synthesis (Reaction 1, industrially known as the Haber-Bosch process):



and water splitting (Reaction 2):



The constant K contours for these reactions can be plotted on the universal colormaps and compared ([Figure 4](#)).³² Using the reaction thermodynamic properties, dimensional parameters (T , P , and E) are shown for each reaction on the secondary axes. In addition to helping visualize the equilibrium constants for these reactions in standard units, these secondary axes demonstrate that the non-dimensional axes span a sufficient range of operating conditions for most reactions. The key points to consider with these plots are: (1) the red dot represents ambient conditions, and the horizontal distance to $\Theta = 0$ is inversely proportional to the enthalpy of reaction; (2) the red vertical line attached to each ambient conditions point on the pressure-temperature plots ([Figures 4A and 4C](#)) represents an increase of an order of magnitude in pressure; (3) the vertical distance from the red dot to the solid pink line ($K = 1$) on the voltage-temperature plots ([Figures 4B and 4D](#)) is the *non-dimensional equilibrium potential* of the reaction.

For the case of ammonia synthesis ([Figures 4A and 4B](#)), the thermodynamic equilibrium favors full conversion of nitrogen and hydrogen to ammonia at ambient conditions; however, kinetics mandate the use of an elevated operating temperature and pressure. This reaction is an important example of the utility of thermodynamic analyses even for reactions where kinetics dictate operating conditions. The scaling of the axes (seen by the secondary axes) demonstrates that crossing equilibrium contours and moving around the thermodynamic equilibrium space with temperature and pressure are feasible at practical operating conditions for ammonia synthesis. In other words, at a temperature at which the kinetics are favorable for ammonia synthesis, the visualization demonstrates that pressure can allow us to easily move through thermodynamic equilibrium space; this is reflected in the fact that ammonia synthesis is commercially practiced at elevated pressures that enable higher equilibrium conversions. This is in contrast with water splitting ([Figures 4C and 4D](#)), for which the visualization clearly demonstrates that increasing pressure decreases conversion, and enormous temperatures are

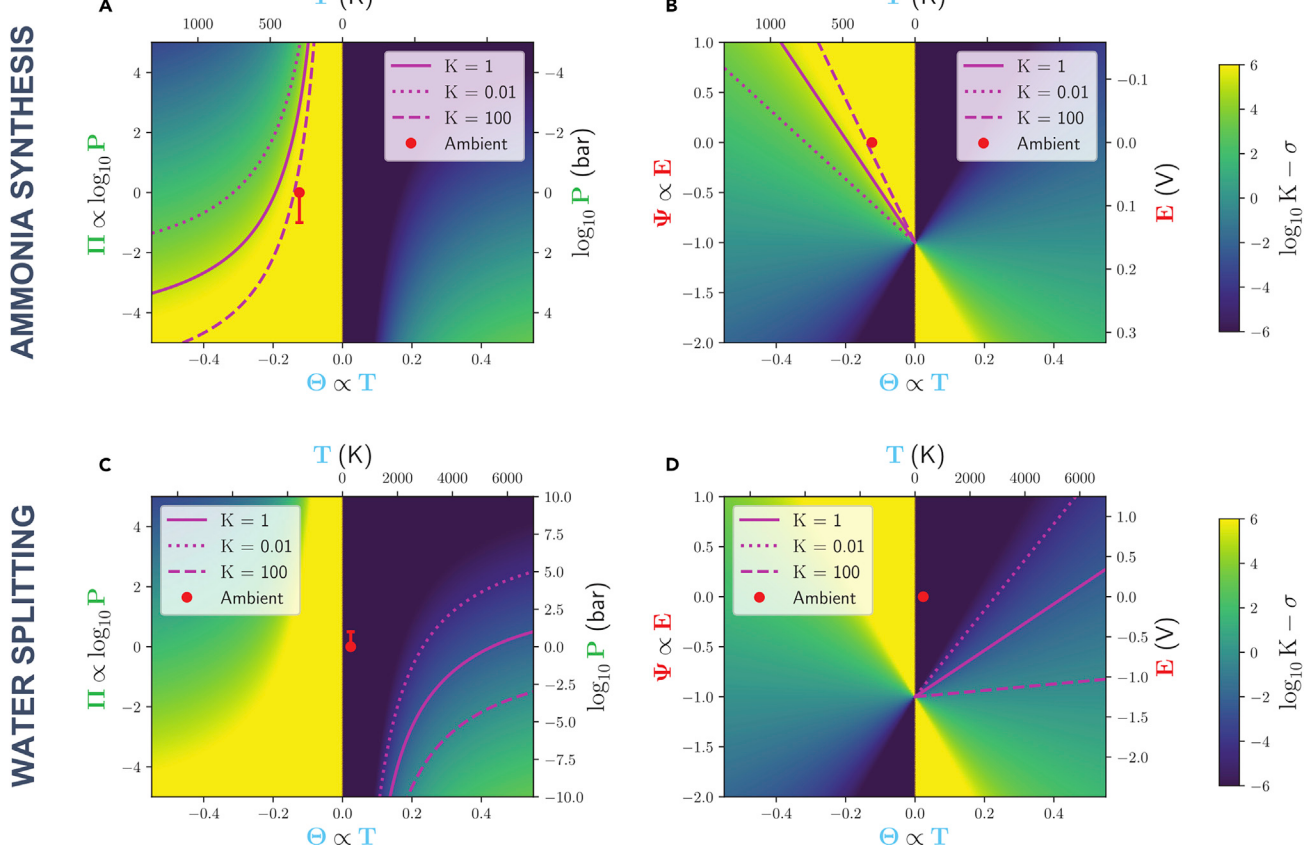


Figure 4. Plots of Equation 4 for Ammonia Synthesis (Reaction 1) and Water Splitting (Reaction 2), Using the Given Stoichiometry

(A–D) Qualitative information about chemical reactions is available from the thermodynamic equilibrium constant as a function of various driving forces. In particular, the equilibrium constant for ammonia synthesis (A and B) and water splitting (C and D) can be compared as functions of pressure and temperature (A and C) and as functions of voltage and temperature (B and D). Pink lines indicate constant K contours for each reaction, the red dots represent ambient conditions, and the vertical line extending from each red point in the thermochemistry plots (A and C) represents an increase in pressure of one order of magnitude. In particular, the horizontal distance from the red dot to $\Theta=0$ is inversely proportional to the enthalpy of reaction, and the vertical distance between the red dot and the solid pink line on the electrochemistry plots (B and D) represents the non-dimensional equilibrium potential. Dimensional thermodynamic parameters on the secondary axes demonstrate that the axes span a sufficient range of operating conditions and are reaction dependent. Dimensional parameters also show how reactions cannot cross $\Theta=0$ since that would correspond to a switch in sign of ΔH_{rxn}^0 , a quantity fixed by the reaction (assuming $\Delta C_{P,rxn} = 0$). Temperature and pressure enable facile movement in thermodynamic space for ammonia synthesis, whereas voltage is necessary to drive water splitting.

necessary to achieve meaningful equilibrium conversions. However, voltage remains a powerful tool, since approximately 1.2 V is sufficient to drive water splitting, a feasible amount compared with the high temperature or low pressure necessary otherwise. This analysis is currently limited to thermodynamic equilibrium considerations, while in reality temperature, pressure, and voltage also play a role in kinetics, cost, selectivity, and safety, all of which strongly influence the trade-offs between thermochemistry and electrochemistry. These other factors are beyond the scope of this analysis as we aim to describe broad trends in driving forces for chemical reactions using a thermodynamic framework. Even without knowledge of these other factors, a thermodynamic analysis reveals whether high conversion is even physically possible, a prerequisite to engineering reactivity given operating conditions dictated by kinetics and other non-thermodynamic constraints. This continues to motivate the search for catalysts that are active at lower temperatures in the case of ammonia synthesis, while telling us not to search

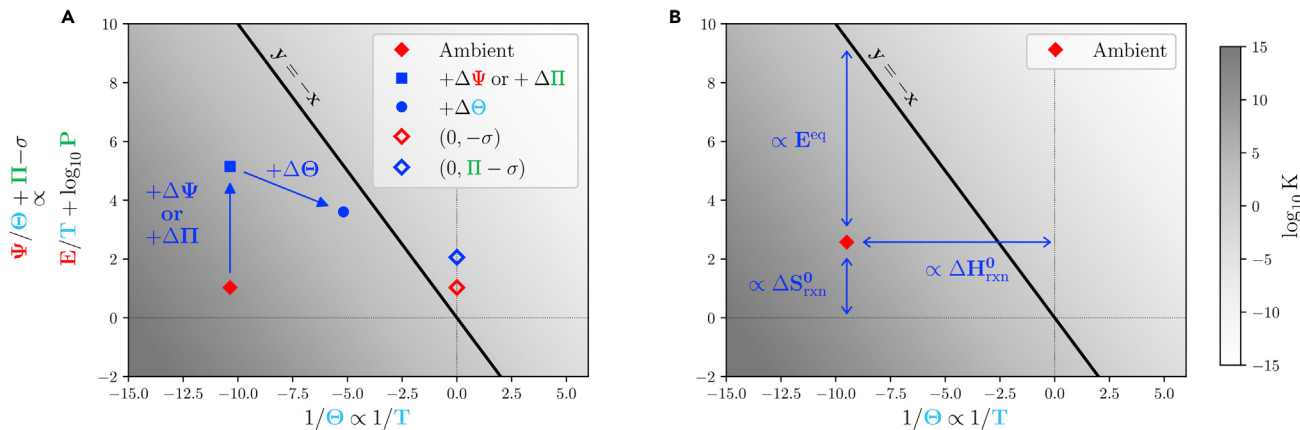


Figure 5. Redefined Axes Such that All Reactions Have the Same Equilibrium K Contours

(A and B) A contour corresponding to $K = 1$ is indicated with a diagonal black line ($y = -x$). The filled red diamonds represent example reaction points at ambient conditions given by Equation 8. An increase in either pressure (Π) or voltage (Ψ) is a vertical movement on these axes (A, new reaction point given by blue square) and an increase in temperature (Θ) is a movement toward the point $(0, \Pi - \sigma)$ (A, new reaction point given by blue circle, movement along the line connecting to the empty blue diamond). As shown, the x coordinate of each point is proportional to ΔH_{rxn}^0 , the y coordinate of each point is proportional to ΔS_{rxn}^0 , and the vertical distance from each point to the solid black line ($K = 1$, given by $y = -x$) is proportional to the dimensional equilibrium potential of the reaction (B). Further details in Derivations S6 and S7.

for thermochemical water splitting catalysts at ambient conditions due to thermodynamic restrictions.

While these universal colormaps are useful for visualizing individual reactions, they are not ideal for comparing multiple reactions because they require unique constant K contours for each reaction, meaning that multiple reactions would quickly obscure each other. Instead, the axes can be redefined such that every reaction has the same K contours, facilitating direct comparison between different reactions.

Visual Comparison and Analysis of Chemical Reactions

Instead of using the non-dimensional groups derived above as axes, in which each reaction has a distinct set of K contours, a simple variable transformation can collapse these to a single set of equilibrium K contours for all reactions (Figure 5). Specifically, the x axis is transformed to $1/\Theta$ and the y axis is transformed to $\Psi/\Theta + \Pi - \sigma$ (Derivation S6). In general, we assume that in addition to temperature, either voltage or pressure is being used to drive the reaction, not both simultaneously, which results in either $\Pi = 0$ or $\Psi = 0$, respectively.

As depicted, in these axes a change in pressure or voltage corresponds to a vertical movement relative to the reaction point and an increase (decrease) in T corresponds to a movement toward (away from) the point $(0, \Pi - \sigma)$ (Figure 5A; Derivation S6). These new, composite axes allow for the direct comparison of chemical reactions since all reactions have the same K contours, with each reaction at ambient conditions represented by a single point:

$$(x, y)_{rxn}^{\text{ambient}} = \left(\frac{1}{\Theta_{\text{ambient}}}, -\sigma \right) \quad (\text{Equation 8})$$

$$= \left(\frac{\Delta H_{rxn}^0}{RT^0 \log_e 10}, - \frac{\Delta S_{rxn}^0}{R \log_e 10} \right),$$

where $T^0 = 298.15$ K. For each reaction point at ambient conditions, the distance from the reaction point to $x=0$ is proportional to ΔH_{rxn}^0 , the distance to $y=0$ is

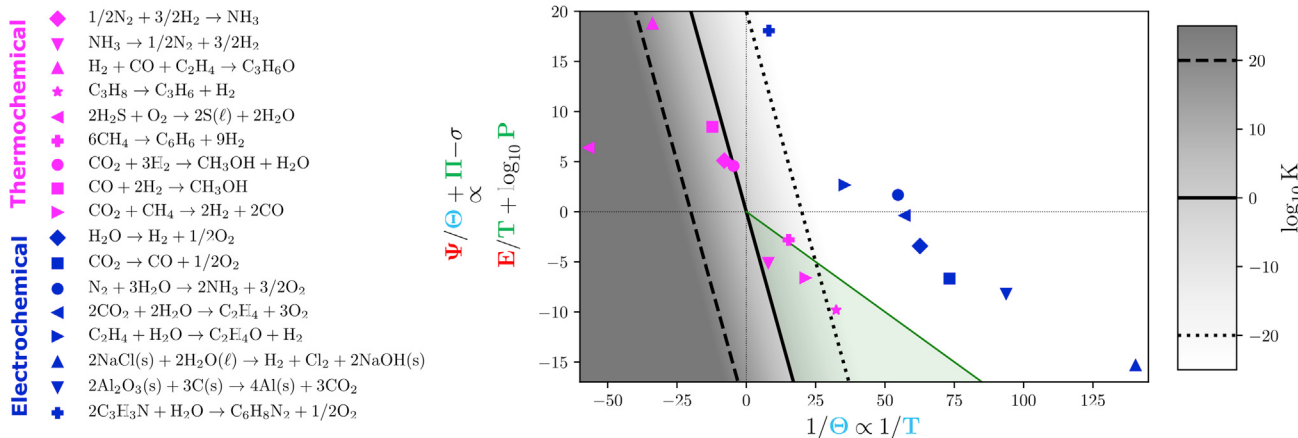


Figure 6. Comparison of Multiple Reactions on the Same Axes

Each point represents a chemical reaction as per Equation 8, with color denoting whether the reaction is typically conducted thermochemically (pink) or electrochemically (blue). Each reaction point is such that $(x, y)^{\text{ambient}} \propto (\Delta H_{\text{rxn}}^0, -\Delta S_{\text{rxn}}^0)$ and can be interpreted as described in Figure 5 (addition of vertical lines representing the effect of pressure analogous to that in Figure 4 and secondary x axis in terms of Θ in Derivation S7). The green shading indicates the area where an elevated temperature of less than $\sim 1,500$ K can reach $K = 1$, and a quantitative visual divide based on reaction enthalpies and entropies distinguishes between reactions driven with electrochemistry versus those driven with thermochemistry. Note that the stoichiometry depicted in the legend is for readability; all reactions have been scaled to have the same number of electrons for best comparison (Derivation S7). To be consistent, chemical formulas were used for all species in the legend, but the following formulas are not unique and refer to the specified chemical: C_3H_6O (propanal), C_2H_4O (ethylene oxide), C_3H_6 (propene), C_6H_6 (benzene), C_3H_3N (acrylonitrile), and $C_6H_8N_2$ (adiponitrile). Raw thermodynamic data given in Data S1 and S2.^{32,36–38}

proportional to ΔS_{rxn}^0 , and the distance to the solid black line ($K = 1$, given by $y = -x$) is proportional to the dimensional equilibrium potential of the reaction (Figure 5B; Derivation S7).

When multiple reactions are plotted on these axes, a clear divide appears between those that are conventionally driven thermochemically versus electrochemically (Figure 6). Reactions to the left of the $K = 1$ line ($y = -x$) are already thermodynamically favorable at ambient conditions. Any adjustment to the reaction conditions (e.g., an increase in temperature to improve kinetics) must keep the reaction as far left as possible to maintain thermodynamic favorability. If the reaction point is near or to the right of the $K = 1$ line ($y = -x$), then pressure or temperature can practically cross the equilibrium contours only if the reaction point is within a reasonable distance to the $K = 1$ line. In particular, to use pressure to drive conversion, the vertical distance from the reaction point to the line $y = -x$ must be within a couple of orders of magnitude of pressure (a version of Figure 6 with pressure effects depicted for each reaction is shown in Derivation S6).

If the reaction point lies to the right of the $K = 1$ line ($y = -x$), then the reaction can be driven to quantifiable conversion using just temperature when the horizontal distance from the reaction point to $y = -x$ is sufficiently small and the reaction point does not lie in the top-right quadrant; in that quadrant, the ΔH_{rxn}^0 and ΔS_{rxn}^0 conspire to make the $K = 1$ contour unreachable with temperature. The horizontal distance to $y = -x$ is quantified by the temperature, T^{eq} , when $K(P = 1 \text{ bar}, T = T^{\text{eq}}) = 1$, namely when $T^{\text{eq}} = \Delta H_{\text{rxn}}^0 / \Delta S_{\text{rxn}}^0$. Due to physical practicalities, the operating temperature should be within a factor of ca. 5 of the ambient temperature (~ 1500 K), a choice which is further discussed in Derivation S8).³³ Mathematically, this translates to $T^{\text{eq}} / T^{\text{ambient}} = 1 / (\sigma \Theta^{\text{ambient}}) \leq 5$. For a reaction point given by $(x, y)^{\text{ambient}}$ on these axes, the reaction can practically be driven by temperature alone when $1 / (\sigma \Theta^{\text{ambient}}) = -x/y \leq 5$, approximately (green shading on Figure 6).

Voltage, however, is particularly well suited to drive chemical reactions that are far from the $K = 1$ line since even large values of Ψ/Θ generally correspond to voltages of order 1 V ([Derivation S4](#)). Thus, this visualization quantitatively supports our intuition, namely that reactions with large, positive values of ΔH_{rxn}^0 (highly endothermic) are generally better driven by voltage. In particular, reactions which require large excursions on these non-dimensional axes can generally only be done electrochemically ([Figure 6](#), blue points). Those requiring small excursions on these axes can generally be done either electrochemically or thermochemically, and these reactions often are driven with temperature and pressure due to industrial expertise and convenience ([Figure 6](#), pink points). For reactions that could be driven either thermochemically or electrochemically, reaction-specific properties such as kinetics and selectivity must be taken into account when choosing a driving force, as well.

Beyond the influence of temperature, pressure, and voltage on the chemical equilibrium, system design choices can also shift the reaction equilibrium. For example, removal of products from the reactor can shift the equilibrium away from reactants (Le Chatelier's principle). Multi-step chemical looping strategies can operate at lower temperatures, which is leveraged in solar thermal water splitting and solar thermal carbon dioxide reduction to drive these reactions at temperatures less than 1,500 K. These multi-step reactions are outside the scope of our present analysis, but it can be extended to understand these systems as well ([Derivation S8](#)).^{34,35} Note that throughout our analysis we restrict ourselves to redox reactions for synthesizing chemicals and do not address reactions where energy is extracted (e.g., via a combustion engine or a fuel cell).

On these proposed axes ([Figure 5](#)), the thermodynamic equilibrium conversion at ambient conditions is readily determined for any reaction by generating a single point (x, y) . Unlike binary descriptors for a chemical reaction such as endo- versus exothermic or sign of ΔG_{rxn} ([Derivation S9](#)), the points representing each reaction can be easily shifted to account for non-ambient conditions (e.g., operating conditions). Additionally, these points inherently encompass multiple discriminating properties of a chemical reaction. First, we can use these points to determine if temperature or pressure can individually drive a reaction to high conversion via the x and y values (see [Derivation S6](#) for more details). Second, we can determine if, at practical operating conditions (e.g., elevated temperatures), other driving forces such as pressure can result in high equilibrium conversion. Last, we can visually discriminate when voltage is necessary for high conversion, recognizing that for cases where temperature, pressure, or voltage all exhibit high fidelity as driving forces for a chemical reaction, significant practical maturity in the use of temperature and pressure as driving forces for a wide range of chemical reactions may favor their usage.

In addition to allowing direct comparison of chemical reactions, these axes also enable facile addition and subtraction of reactions. For example, both water splitting (blue diamond) and ammonia synthesis (pink diamond) are represented, but the sum of these two reactions, converting water and nitrogen to ammonia and oxygen, is also shown (blue circle) and has (x, y) coordinates that are simply the sum of the two individual reaction points ([Figure 6](#)). This is a manifestation of Hess's Law, namely that the total enthalpy change for a reaction given by multiple steps is the sum of all enthalpy changes of the individual steps. Combining reactions on these axes to generate new reactions is therefore simple and enables quick visual analysis of how multiple reactions can work together from a thermodynamic perspective. This additive property of these axes makes it clear why using water as a source of hydrogen or oxygen can be difficult with pressure and temperature but is feasible with voltage as a driving force; since the water splitting point is so far from the

vertical axis (very endothermic), the specific reaction where we want to replace hydrogen or oxygen would need to be equally far on the opposite side of $x = 0$ to be thermochemically feasible using water as a reactant.

Conclusions

Beginning with the question: "why should a given chemical reaction be driven preferentially with temperature (thermal energy), pressure (mechanical energy), or voltage (electrical energy)?" we developed a non-dimensional, reaction-independent expression for chemical equilibrium as a function of thermodynamic driving forces. We then analyzed the thermodynamics for multiple industrial and lab-scale chemical reactions that rely on different combinations of temperature, pressure, and voltage as driving forces and compared them visually on the same axes, finding a clear discrimination between electrochemically and thermochemically driven reactions. Converting from temperature, pressure, and voltage to heat and work fluxes reveals that our analysis has a strong physical basis in work and energy exchanges.

The universal equation and facile visualization of chemical reactions provide both a quantitative framework for comparing thermodynamic driving forces as well as an intuitive platform for comparing multiple reactions. However, chemical reaction conditions are often dictated by more than just thermodynamics and require knowledge of kinetics, selectivity, costs, and associated unit operations, such as those involved in separations. Other parameters such as reactant availability, the possibility of modular and distributed manufacturing, and safety are also necessary considerations. Thus, the decision between using traditional heat and mechanical work to drive a reaction versus using electricity in reality depends on much more than the thermodynamics. However, academic and industrial research on chemical reactions often begins long before estimates of practical operating parameters are available. The quantitative thermodynamic framework presented here allows comparison of candidate reactions and driving forces at the early stages of developing new reactions and processes, before a process is sufficiently mature to inform detailed techno-economic and safety analyses.

EXPERIMENTAL PROCEDURES

Resource Availability

Lead Contact

Further information and requests for resources and materials should be directed to and will be fulfilled by the Lead Contact, Karthish Manthiram (karthish@mit.edu).

Materials Availability

This study did not generate new unique materials.

Data and Code Availability

The code generated during this study are available at Zenodo via <https://doi.org/10.5281/zenodo.4314075>.

Thermodynamic data were taken from NIST,³² the Dortmund Data Bank,³⁶ Lange's Handbook of Chemistry,³⁷ and group additivity theory via RMG³⁸ depending on availability, with the most recent data point used if multiple data points were provided (raw data provided in [Table S1](#)). Derivations for all analytical thermodynamic expressions shown in the main text are provided in the [Derivations S6](#) and [S7](#). Starting with the expression for an equilibrium constant ([Equation 3](#)), we derived an expression that explicitly included the dependence on specific driving forces of

interest (pressure, temperature, and voltage). This expression was then non-dimensionalized in preparation for better comparison and visualization. Energy and work exchanges were calculated by conducting energy and entropy balances. Analysis and visualization of all data was performed using Python and matplotlib.

SUPPLEMENTAL INFORMATION

Supplemental Information can be found online at <https://doi.org/10.1016/j.joule.2020.12.014>.

ACKNOWLEDGMENTS

This material is based on work supported by the National Science Foundation under grant no. 1944007. The authors thank Nathan Corbin, Nikifar Lazouski, and Kindle Williams for useful discussions. Z.J.S. and A.M.L. also acknowledge a graduate research fellowship from the National Science Foundation under grant no. 1745302.

AUTHOR CONTRIBUTIONS

Conceptualization, Z.J.S. and K.M.; Methodology, Z.J.S., A.M.L., and K.M.; Software, Z.J.S.; Validation, Z.J.S., A.M.L., and K.M.; Investigation, Z.J.S., A.M.L., and K.M.; Resources, Z.J.S., A.M.L., and K.M.; Writing – Original Draft, Z.J.S.; Writing – Review & Editing, Z.J.S., A.M.L., and K.M.; Visualization, Z.J.S.; Supervision, K.M.; Funding Acquisition, K.M.

DECLARATION OF INTERESTS

The authors declare no competing interests.

Received: September 13, 2020

Revised: November 11, 2020

Accepted: December 16, 2020

Published: January 11, 2021

REFERENCES

1. EIA (2016). International energy outlook 2016. Technical report of the U.S. Energy Information Administration. May 2016. <https://www.osti.gov/biblio/1296780>.
2. IEA; ICCA; DECHEMA (2013). Technology roadmap: energy and GHG reductions in the chemical industry via catalytic processes. Technical report of the IEA, ICCA, and DECHEMA. June 2013. <https://www.iea.org/reports/technology-roadmap-energy-and-ghg-reductions-in-the-chemical-industry-via-catalytic-processes>.
3. Friend, C.M., and Xu, B. (2017). Heterogeneous catalysis: a central science for a sustainable future. *Acc. Chem. Res.* 50, 517–521.
4. Arora, A., and Gambardella, A. (2011). Implications for energy innovation from the chemical industry. In *Accelerating Energy Innovation: Insights from Multiple Sectors* (University of Chicago Press), pp. 87–111.
5. van Geem, K.M., Galvita, V.V., and Marin, G.B. (2019). Making chemicals with electricity. *Science* 364, 734–735.
6. Gu, S., Xu, B., and Yan, Y. (2014). Electrochemical energy engineering: a new frontier of chemical engineering innovation. *Annu. Rev. Chem. Biomol. Eng.* 5, 429–454.
7. Schnuelle, C., Thoeming, J., Wassermann, T., Thier, P., von Gleich, A. v., and Goessling-Reisemann, S. (2019). Socio-technical-economic assessment of power-to-X: potentials and limitations for an integration into the German energy system. *Energy Res. Soc. Sci.* 51, 187–197.
8. Schiffer, Z.J., and Manthiram, K. (2017). Electrification and decarbonization of the chemical industry. *Joule* 1, 10–14.
9. Botte, G.G. (2014). Electrochemical manufacturing in the chemical industry. *Interface Mag.* 23, 49–55. https://www.electrochem.org/dl/interface/fal/fal14_fal14_p049_055.pdf.
10. Wang, Z., Roberts, R.R., Naterer, G.F., and Gabriel, K.S. (2012). Comparison of thermochemical, electrolytic, photoelectrolytic and photochemical solar-to-hydrogen production technologies. *Int. J. Hydr. Energy* 37, 16287–16301.
11. Jouny, M., Luc, W., and Jiao, F. (2018). General techno-economic analysis of CO₂ electrolysis systems. *Ind. Eng. Chem. Res.* 57, 2165–2177.
12. Zhao, Y., Setzler, B.P., Wang, J., Nash, J., Wang, T., Xu, B., and Yan, Y. (2019). An efficient direct ammonia fuel cell for affordable carbon-neutral transportation. *Joule* 3, 2472–2484.
13. Na, J., Seo, B., Kim, J., Lee, C.W., Lee, H., Hwang, Y.-J., Min, B.K., Lee, D.K., Oh, H.S., and Lee, U. (2019). General technoeconomic analysis for electrochemical coproduction coupling carbon dioxide reduction with organic oxidation. *Nat. Commun.* 10, 5193.
14. Müller, K., Brooks, K., and Autrey, T. (2017). Hydrogen storage in formic acid: a comparison of process options. *Energy Fuels* 31, 12603–12611.
15. Jouny, M., Hutchings, G.S., and Jiao, F. (2019). Carbon monoxide electroreduction as an emerging platform for carbon utilization. *Nat. Cat.* 2, 1062–1070.
16. Verma, S., Lu, S., and Kenis, P.J.A. (2019). Co-electrolysis of CO₂ and glycerol as a pathway to carbon chemicals with improved technoeconomics due to low electricity consumption. *Nat. Energy* 4, 466–474.
17. Carnot, S. (1824) *Réflexions Sur La Puissance Motrice du Feu et Sur Les Machines Propres à Développer Cette Puissance* (Paris).

18. Smeaton, J. (1759). XVIII. An experimental enquiry concerning the natural powers of water and wind to turn mills, and other machines, depending on a circular motion. *Philos. Trans. R. Soc. Lond.* 51, 100–174.
19. Hoffmann, K.H. (2008). An introduction to endoreversible thermodynamics. Proceedings of the International Conference and Summer School on Thermal Theories of CONTINUA: Survey and Developments, 86, pp. 1–18.
20. Andresen, B., Berry, R.S., Nitzan, A., and Salamon, P. (1977). Thermodynamics in finite time. I. The step-Carnot cycle. *Phys. Rev. A* 15, 2086–2093.
21. Sieniutycz, S., and Jeżowski, J. (2018). Energy limits for thermal engines and heat pumps at steady states. In *Energy Optimization in Process Systems and Fuel Cells* (Elsevier), pp. 81–119.
22. Inzelt, G. (2015). Crossing the bridge between thermodynamics and electrochemistry. From the potential of the cell reaction to the electrode potential. *ChemTexts* 1, 1–11.
23. Keszei, E. (2011). *Chemical Thermodynamics: An Introduction*, Twelfth Edition (Springer).
24. Clarke, E.C.W., and Glew, D.N. (1966). Evaluation of thermodynamic functions from equilibrium constants. *Trans. Faraday Soc.* 62, 539–547.
25. Bockris, J.O. (1981). *Comprehensive Treatise of Electrochemistry Vol. 3: Electrochemical Energy Conversion and Storage*, First Edition (Springer).
26. Hecksher, T. (2017). Insights through dimensions. *Nat. Phys.* 13, 1026.
27. Meixner, J. (1975). Coldness and temperature. *Arch. Rational Mech. Anal.* 57, 281–290.
28. Bazhin, N.M. (2011). Mechanism of electric energy production in galvanic and concentration cells. *J. Engin. Thermophys.* 20, 302–307.
29. Bazhin, N.M., and Parmon, V.N. (2007). Conversion of the chemical reaction energy into useful work in the Van't Hoff equilibrium box. *J. Chem. Educ.* 84, 1053–1055.
30. Kowalewicz, A. (2001). Fuel-cell: power for future. *J. KONES* 8, 325–333.
31. Panagiotopoulos, A.Z. (2011). *Essential Thermodynamics*, First Edition (CreateSpace Independent Publishing Platform).
32. Burgess, D. (2020). Thermochemical data. Thermochemical data. In *NIST Chemistry WebBook*, NIST Standard Reference Database Number 69, P. Linstrom and W. Mallard, eds., chapter Thermochem. National Institute of Standards and Technology Gaithersburg. (MD).
33. Weissmel, K., and Arpe, H. (2003). *Industrial Organic Chemistry*, Fourth Edition (Wiley-VCH Verlag).
34. Hao, Y., Yang, C.-K., and Haile, S.M. (2014). Ceria-zirconia solid solutions ($\text{Ce}_{1-x}\text{Zr}_x\text{O}_2-\delta$, $x \leq 0.2$) for solar thermochemical water splitting: a thermodynamic study. *Chem. Mater.* 26, 6073–6082.
35. Furler, P., Scheffe, J., Gorbar, M., Moes, L., Vogt, U., and Steinfeld, A. (2012). Solar thermochemical CO_2 splitting utilizing a reticulated porous ceria redox system. *Energy Fuels* 26, 7051–7059.
36. Dortmund Data Bank. (2020). www.ddbst.com.
37. Lange, N.A. (1999). *Lange's Handbook of Chemistry*, Fifteenth Edition (McGraw-Hill, Inc).
38. Gao, C.W., Allen, J.W., Green, W.H., and West, R.H. (2016). Reaction mechanism generator: automatic construction of chemical kinetic mechanisms. *Comput. Phys. Commun.* 203, 212–225.

JOUL, Volume 5

Supplemental Information

**Thermodynamic Discrimination
between Energy Sources for Chemical Reactions**

Zachary J. Schiffer, Aditya M. Limaye, and Karthish Manthiram

Contents

Supplemental Data	S-1
S1 Raw data for chemical species	S-1
S2 Raw reaction thermodynamics for reaction equations	S-2
Supplemental Experimental Procedures	S-3
S1 Equilibrium constant	S-3
S2 Relationship between equilibrium constant K and conversion	S-6
S3 Non-dimensionalization of equilibrium expression	S-7
S4 Constant K contours and comparison of driving forces	S-8
S5 Derivation of work and energy exchange	S-11
S6 Redefinition of axes to collapse K contours	S-16
S7 Scaling of reaction stoichiometry to compare reactions	S-17
S8 Quantitative limits on thermochemical and electrochemical reactions	S-19
S9 Simple Descriptors	S-20
Supplemental References	S-22

Supplemental Data

S1 Raw data for chemical species

Table S1: Molecule raw thermodynamic parameters. These raw values are used to generate the reaction enthalpies and entropies used in the main text (primarily Figure 6).

Molecule	ΔH_f^0 (kJ/mol) ^a	S_f^0 (J/mol.K) ^a	Phase
CO ₂	-393.52	213.79	g
CO	-110.53	197.66	g
CH ₄	-74.6	186.25	g
H ₂ O	-241.83	188.84	g
H ₂ O	-285.83	69.95	ℓ
MeOH	-205	239.81 ^c	g
H ₂	0	130.68	g
N ₂	0	191.61	g
O ₂	0	205.15	g
NH ₃	-45.9	192.77	g
Al ₂ O ₃	-1675.69	50.92	s
C ^b	0	5.6	s
Al	0	28.3	s
NaCl	-411.12	72.11	s
Cl ₂	0	223.08	g
NaOH	-425.93	64.46	s
Propanal	-188.7	304.4	g
C ₂ H ₄	52.4	219.32	g
C ₂ H ₆	-84.0	229.1 ^d	g
H ₂ S	-20.5	205.77	g
S	1.85	36.85	ℓ
S	276.98	167.83	g
Benzene	82.9	269.2 ^d	g
Ethylene Oxide	-52.64	243.00	g
Acrylonitrile	179.7	274.1 ^d	g
Adiponitrile	149	400.5 ^e	g
C ₃ H ₈	-104.7	270.2 ^d	g
Propene	20.41	266.6 ^d	g

^a Data from NIST unless otherwise specified¹

^b Data for graphite

^c Data from Dortmund Data Bank²

^d Data from Lange's Handbook of Chemistry³

^e Data from RMG using group additivity⁴

S2 Raw reaction thermodynamics for reaction equations

Table S2: Reaction raw thermodynamic parameters. These are the reaction thermochemical parameters used throughout this work (primarily Figure 6). The stoichiometry is normalized as described in Section S7 and the raw data for individual molecules is provided in Table S1.

Reaction Stoichiometry	ΔH_{rxn}^0 (kJ/mol)	ΔS_{rxn}^0 (J/mol.K)	$\sum_{i \in \text{gas}} \nu_i$	n_{e^-}
$\frac{1}{2} \text{N}_2 + \frac{3}{2} \text{H}_2 \longrightarrow \text{NH}_3$	-45.9	-99.1	-1	3
$\text{NH}_3 \longrightarrow \frac{1}{2} \text{N}_2 + \frac{3}{2} \text{H}_2$	45.9	99.1	1	3
CHECK $\text{H}_2 + \text{CO} + \text{C}_2\text{H}_4 \longrightarrow \text{Propanal}$	-130.7	-243.3	-2	2
Propane \longrightarrow Propylene + H_2	125.1	127.1	1	2
$2 \text{H}_2\text{S} + \text{O}_2 \longrightarrow 2 \text{S}(\ell) + 2 \text{H}_2\text{O}$	-439.0	-165.3	-1	4
$6 \text{CH}_4 \longrightarrow \text{Benzene} + 9 \text{H}_2$	530.5	327.8	4	18
$\text{CO}_2 + 3 \text{H}_2 \longrightarrow \text{CH}_3\text{OH} + \text{H}_2\text{O}$	-53.3	-177.2	-2	6
$\text{CO} + 2 \text{H}_2 \longrightarrow \text{CH}_3\text{OH}$	-94.5	-219.2	-2	4
CHECK $6 \text{CO}_2 + \text{CH}_4 \longrightarrow 2 \text{H}_2 + 2 \text{CO}$	247.0	256.6	2	6
$\text{H}_2\text{O} \longrightarrow \text{H}_2 + \frac{1}{2} \text{O}_2$	241.8	44.4	0.5	2
$\text{CO}_2 \longrightarrow \text{CO} + \frac{1}{2} \text{O}_2$	283.0	86.4	0.5	2
$\text{N}_2 + 3 \text{H}_2\text{O} \longrightarrow 2 \text{NH}_3 + \frac{3}{2} \text{O}_2$	633.7	-64.9	-0.5	6
$2 \text{CO}_2 + 2 \text{H}_2\text{O} \longrightarrow \text{C}_2\text{H}_4 + 3 \text{O}_2$	1323.2	29.5	0	12
$\text{C}_2\text{H}_4 + \text{H}_2\text{O} \longrightarrow$	136.7	-34.5	0	2
Ethylene Oxide + H_2				
$2 \text{NaCl(s)} + 2 \text{H}_2\text{O}(\ell) \longrightarrow$	542.0	198.6	2	2
$\text{H}_2 + \text{Cl}_2 + 2 \text{NaOH(s)}$				
$2 \text{Al}_2\text{O}_3(\text{s}) + 3 \text{C(s)} \longrightarrow$	2170.9	635.9	3	12
$4 \text{Al(s)} + 3 \text{CO}_2$				
$2 \text{Acrylonitrile} + \text{H}_2\text{O} \longrightarrow$	31.4	-233.9	-1.5	2
Adiponitrile + $\frac{1}{2} \text{O}_2$				

Supplemental Experimental Procedures

S1 Equilibrium constant

As in the main text, we will start with a generic chemical equation and a statement of equilibrium at constant T , P , and E :

$$\sum_i \nu_i A_i = 0 \quad (\text{S1})$$

$$\sum_i \nu_i \mu_i(T, P, E) = 0 \quad (\text{S2})$$

Here, ν_i is the stoichiometric coefficient for chemical species A_i and μ_i is the *electrochemical* potential. The influence of applied potential on our system can be expressed as,

$$\sum_i \nu_i \mu_i(T, P, E) = \sum_i \nu_i \bar{\mu}_i(T, P) + n_{e^-} F E = 0 \quad (\text{S3})$$

where n_{e^-} is the minimum number of electrons necessarily transferred in the reaction, F is Faraday's constant, and $\bar{\mu}_i(T, P)$ is the *chemical* potential of species i . Note that in theory, convoluted half-reactions and reaction design can allow for an arbitrary number of electrons to be transferred, but we choose the minimum possible number of electrons given a reaction stoichiometry in order for n_{e^-} to have a unique value for each overall reaction stoichiometry (choice of stoichiometry discussed in Supplemental Derivation S7).

We can express the chemical potentials ($\bar{\mu}_i$) in terms of the activities (a_i) and the chemical potentials of the ideal pure substance ($\bar{\mu}_i^0(T, P^0)$),

$$\bar{\mu}_i(T, P) = \bar{\mu}_i^0(T, P^0) + RT \log_e a_i \quad (\text{S4})$$

We can set our reference states such that $\bar{\mu}_i^0(T, P^0) = \Delta G_f(T, P^0)$ (the Gibbs Free Energies of formation). In addition, we are dealing with an ideal gas mixture—therefore $a_i = p_i/P^0 = y_i P/P^0$, where p_i are the partial pressures and y_i are the mole fractions of the components.

Plugging in, we get the following result:

$$0 = \sum_i \nu_i \mu_i(T, P, E) \quad (\text{S5})$$

$$= n_{e^-} F E + \sum_i \left[\nu_i \Delta G_f(T, P^0) + \nu_i R T \log_e \frac{p_i}{P^0} \right] \quad (\text{S6})$$

$$= n_{e^-} F E + \Delta G_{\text{rxn}}(T, P^0) + R T \log_e \frac{P}{P^0} \sum_i \nu_i + R T \sum_i \nu_i \log_e y_i \quad (\text{S7})$$

$$0 = n_{e^-} F E + \Delta H_{\text{rxn}}(T^0, P^0) - T \Delta S_{\text{rxn}}(T^0, P^0) + R T \Delta n_{\text{rxn}} \log_e \frac{P}{P^0} + R T \log_e K \quad (\text{S8})$$

Note we have introduced the variable $K \equiv \prod_{i \in \text{gas}} y_i^{\nu_i}$. We have implicitly used the assumption that $\Delta G_{\text{rxn}}(T, P^0) = \Delta H_{\text{rxn}}(T^0, P^0) - T \Delta S_{\text{rxn}}(T^0, P^0)$. In practice, one will use the Gibbs-Helmholtz equation to find $\Delta G_{\text{rxn}}(T, P^0)$ as a function of temperature. If we assume that $\Delta H_{\text{rxn}}(T, P^0)$ and $\Delta S_{\text{rxn}}(T, P^0)$ are not functions of temperature (equivalently that $\Delta C_{P,\text{rxn}} = 0$), then the expression used here is accurate. Rearranging the above and taking $P^0 = 1$ bar, we get the result from the main text:

$$\log_e K = -\frac{\Delta H_{\text{rxn}}^0}{R T} - \frac{n_{e^-} F E}{R T} - \Delta n_{\text{rxn}} \log_e \frac{P}{1 \text{ bar}} + \frac{\Delta S_{\text{rxn}}^0}{R} \quad (\text{S9})$$

Relaxing our assumption $\Delta C_{P,\text{rxn}} = 0$ so that $\Delta C_{P,\text{rxn}} = \text{const.}$ changes our expression to the following,

$$\begin{aligned} \log_e K &= -\frac{\Delta H_{\text{rxn}}^0}{R T} - \frac{\Delta C_{P,\text{rxn}}^0(T - T^0)}{R T} - \frac{n_{e^-} F E}{R T} \\ &\quad - \Delta n_{\text{rxn}} \log_e \frac{P}{1 \text{ bar}} + \frac{\Delta S_{\text{rxn}}^0}{R} + \frac{\Delta C_{P,\text{rxn}}^0}{R} \log_e \frac{T}{T^0} \\ \log_e K &= -\frac{\Delta H_{\text{rxn}}^0}{R T} - \delta_1 - \frac{n_{e^-} F E}{R T} - \Delta n_{\text{rxn}} \log_e \frac{P}{1 \text{ bar}} + \frac{\Delta S_{\text{rxn}}^0}{R} + \delta_2 \end{aligned} \quad (\text{S10})$$

We could relax this assumption even further such that $\Delta C_{P,rxn} = f(T)$, but this would needlessly complicate our equation and has only second order effects on the result for the operating conditions and reactions we are generally considering (Figure S1). In Equation (S10), we have introduced two new terms: δ_1 and δ_2 . $\delta_2 \propto \log_e T/T^0$, and for $T < \sim 1500$ K = $5T^0$ this term will be approximately $\frac{\Delta C_{P,rxn}^0}{R}$. δ_1 can be analyzed two ways. The first is that it will have two effects: (1) it will add an additional constant term ($\frac{\Delta C_{P,rxn}^0}{R}$) to the equilibrium expression and it will change the “effective” enthalpy of reaction by $\Delta C_{P,rxn}^0 T^0$, likely a small value if $\Delta C_{P,rxn}^0$ is close to zero. The second way δ_1 can be analyzed will be through the lens that $T^0 < T < \sim 1500$ K = $5T^0$. Accordingly, $0 < \delta_1 < \frac{4}{5} \frac{\Delta C_{P,rxn}^0}{R}$. Because δ_1 and δ_2 are subtracted and added to Equation (S10), respectively, we see that together they actually result in a negligible contribution to our expression that qualitatively changes nothing about our results as long as $\Delta C_{P,rxn}^0 \ll \Delta H_{rxn}^0$.

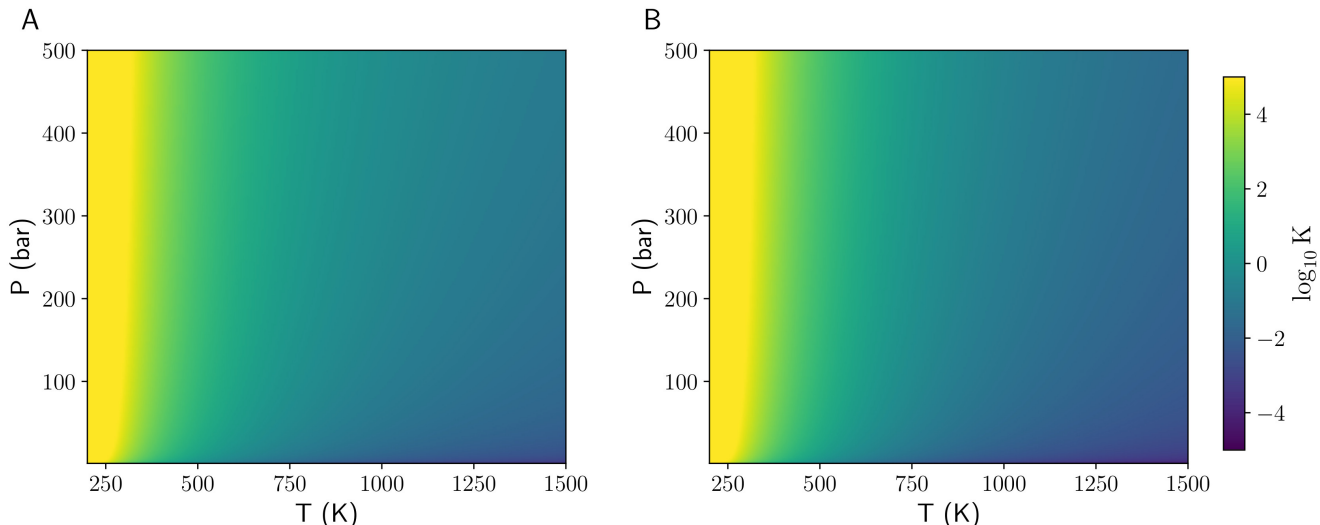


Figure S1: Comparison of equilibrium constant for ammonia synthesis reaction (Equation R1) given the assumptions in the main text (A) and for “real” thermodynamic data taken from NIST (B)¹. They are qualitatively the same, and quantitatively the real equilibrium constant is less than 0.8 logarithmic units lower than it is with our assumptions even at 1500 K.

We have assumed that all of our species are gas phase. If we have species that are liquids or solids, we can replace the activities $a_i = 1$, which results in $\Delta n_{rxn} = \sum_{i \in gas} \nu_i$ and K is only a function of the mole fractions in the gas phase.

To adjust for solvated species reactions, we would change the activity to be a concentration (c_i) instead of a partial pressure and our equilibrium constant would be a function of the system volume. This is beyond the scope of this work but remains a useful exercise for understanding solvated systems which are ubiquitous to electrochemistry.

S2 Relationship between equilibrium constant K and conversion

As mentioned in the main text, we generally are looking for a value for the thermodynamic conversion, $z \in [0, 1]$, when analyzing a reaction since conversion is a much more meaningful quantity to work with when designing reactors than an equilibrium constant. Unfortunately, each reaction will have a slightly different expression for conversion as a function of the equilibrium constant, $z = z(K)$, depending on the stoichiometry. However, there are some commonalities in all of these conversion functions that mean that using K as a proxy for conversion is reasonable. We have shown a couple functions for conversion in terms of the equilibrium constant (Figure S2), where the strict increasing nature of the conversion function is evident. Conversion will in general always be a sigmoidal, increasing function of K , similar to the logistic function ($\text{logit}(x) = \frac{1}{1+e^{-x}}$). Moreover, z will generally span the full range from 0 to 1 in the domain $-5 < \log_{10} K < 5$ regardless of stoichiometry. Because we are normalizing our stoichiometries (Discussion S7), our conversion functions are even more likely to have a similar shape and range.

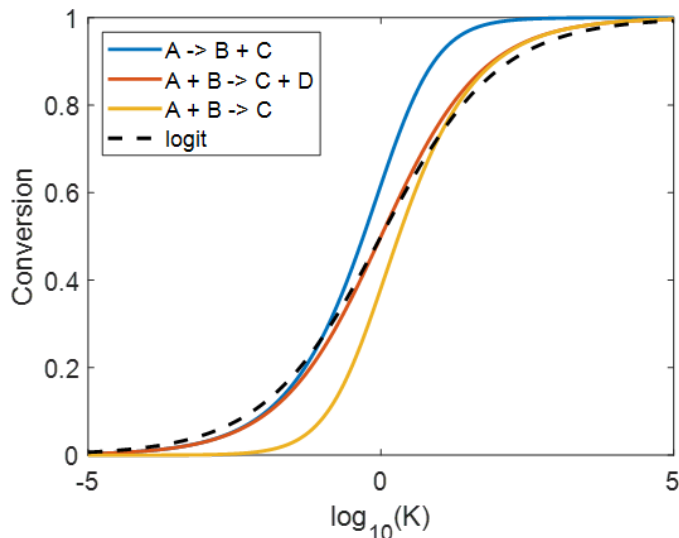


Figure S2: One of the main assumptions the analysis relies upon is that the equilibrium constant (K) is a proxy for conversion. Here, the conversion as a function of the equilibrium constant is shown for multiple different reaction stoichiometries assuming initial stoichiometric quantities of reactants and zero products (solid lines) as well as for the logistic function, logit. As can be seen, conversion is strictly increasing and generally has a similar sigmoidal shape as a function of K for any reaction stoichiometry. Therefore, K is a reasonable proxy for conversion.

In order to derive an exact expression for z as a function of K given a reaction stoichiometry, we will use the common RICE method (Reaction, Initialization, Change, Equilibrium). For example,

We can then write an expression for $K = \prod_i y_i$ and solve for conversion, $z = \epsilon$, as a function of K algebraically or numerically.

Table S3: RICE method for $A + B \rightarrow C + D$

R	A	B	C	D
I	1	1	0	0
C	$-\epsilon$	$-\epsilon$	ϵ	ϵ
E	$1 - \epsilon$	$1 - \epsilon$	ϵ	ϵ

S3 Non-dimensionalization of equilibrium expression

In general, there are multiple ways to non-dimensionalize Equation (S9). When working with partial differential equations, such as the Navier-Stokes equation, non-dimensionalization involves rescaling every quantity by some physical characteristic property so that the variables are order 1 and dimensionless groups such as the Reynolds number are prefactors to parts of the equation. These dimensionless groups make experimental probing of a system simpler since the number of parameters affecting the system has been reduced, and they also make the practical aspects of solving the equations easier either analytically or numerically. In our case, however, we do not have a differential equation, and we want to find an expression for $\log_{10} K$ that is independent of the exact chemical reaction.

Our system is not so amenable to pulling out a simple non-dimensional grouping, so we instead focus on finding characteristic physical parameters that can remove any reaction-specific information from our expression. Our first parameter is temperature. There are multiple options for a characteristic temperature, which we will briefly discuss. The first is $T_{\text{char}} = \Delta H_{\text{rxn}}^0 / \Delta S_{\text{rxn}}^0$. This characteristic temperature is essentially the temperature at which $K = 1$ and pops out from $0 = \Delta G_{\text{rxn}}^0 = \Delta H_{\text{rxn}}^0 - T_{\text{char}} \Delta S_{\text{rxn}}^0$. However, this temperature is not ideal because it can be negative, and for reactions that are thermodynamically favored at ambient conditions, this value provides a poor scaling for the operating temperature. If we instead look directly at Equation (S9), we see that the first term has a natural characteristic temperature already in it: $T_{\text{char}} \equiv \Delta H_{\text{rxn}}^0 / R$. This additionally provides us with a natural energy scaling, ΔH_{rxn}^0 . Of course, this brings up the question, why not use ΔG_{rxn}^0 as an energy scaling since it is perhaps a more relevant quantity for reaction conversion? Unfortunately, using the Gibbs free energy as our characteristic energy results in a needlessly complicated expression for K that makes the entire analysis less intuitive. One last detail is that we chose to define our non-dimensional temperature quantity as $\propto T$ instead of $\propto 1/T$ because the scaling is more intuitive with the direct proportionality.

Given a characteristic energy scaling, a characteristic voltage is simply, $E_{\text{char}} \equiv \frac{\Delta H_{\text{rxn}}^0}{n_e F}$.

The last parameter we need to take care of is pressure. Pressure is different from the rest because it already has a characteristic pressure (the reference pressure, 1 bar) built into the equilibrium expression. However, we still want to remove any dependence on Δn_{rxn} . If we did not want to include the logarithm in our non-dimensional quantity, we would end up with $\Pi = \left(\frac{P}{P^0}\right)^{\Delta n_{\text{rxn}}}$. This, however, is even less intuitive of a non-dimensional pressure than simply wrapping up the entire term into a non-dimensional quantity. As a result, including a change of base so that our expression is in base 10 instead of base e , we get the following

expressions from the main text:

$$\Theta \equiv \frac{RT \log_e 10}{\Delta H_{\text{rxn}}^0}, \quad (\text{S11})$$

$$\Pi \equiv \Delta n_{\text{rxn}} \log_{10} \frac{P}{P^0}, \quad (\text{S12})$$

$$\Psi \equiv \frac{n_{e^-} F E}{\Delta H_{\text{rxn}}^0}, \quad (\text{S13})$$

$$\sigma \equiv \frac{\Delta S_{\text{rxn}}}{R \log_e 10}, \quad (\text{S14})$$

$$\boxed{\log_{10} K = -\frac{1}{\Theta} - \frac{\Psi}{\Theta} - \Pi + \sigma.} \quad (\text{S15})$$

While this justification for non-dimensional groupings may appear slightly arbitrary, it not only results in a simple equilibrium expression but also has a physical basis in the work and heat exchanges with our system, as discussed in the main text.

S4 Constant K contours and comparison of driving forces

Our non-dimensional equation is:

$$\log_{10} K = -\frac{1}{\Theta} - \frac{\Psi}{\Theta} - \Pi + \sigma \quad (\text{S16})$$

We can see that the level curves for a given K at no applied potential ($\Psi = 0$) result in an inverse relationship between Π (base 10 logarithm of pressure) and Θ (temperature):

$$\Pi = (\sigma - \log_{10} K) - \frac{1}{\Theta} \quad (\text{S17})$$

Similarly, we can see that the level curves for a given K at ambient pressure ($\Pi = 0$) result in a linear relationship between Ψ (potential) and Θ (temperature):

$$\Psi = \Theta (\sigma - \log_{10} K) - 1 \quad (\text{S18})$$

Last, we can see that the level curves for a given K at ambient temperature ($\Theta = \Theta^{\text{ambient}}$) result in a linear relationship between Ψ (potential) and Π (pressure):

$$\Pi = -\frac{1}{\Theta^{\text{ambient}}} (1 + \Psi) - \log_{10} K + \sigma \quad (\text{S19})$$

These are the equations used to draw constant K contours in the main text (reproduced in Figure S4). Note that the constant K contours for a pressure-voltage relationship are not reaction-independent due to the appearance of Θ^{ambient} , such that this cannot be plotted in universal form, as we are able to do in the two other cases (Figure S3). Because a voltage-pressure plot is not generalizable to all chemical reactions, we do not discuss it in detail and assume that our system relies on either voltage as a driving force ($\Pi = 0$) or pressure as a driving force ($\Psi = 0$), but not both simultaneously.

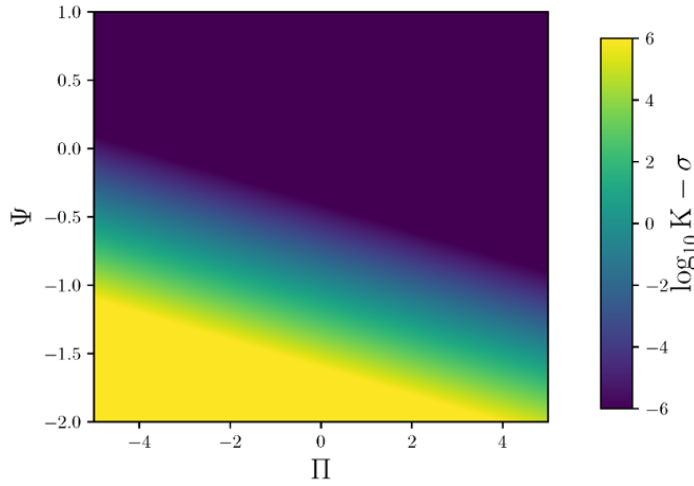


Figure S3: Pressure-voltage contour plot with $\Theta^{\text{ambient}} = 0.1$. Unlike the pressure-temperature and voltage-temperature plots, a pressure-voltage plot depends Θ^{ambient} which means it depends on ΔH_{rxn} (Equation S15). For this reason, it is not a universal colormap and we have included it here for completeness of visualization only. $\Theta^{\text{ambient}} = 0.1$ was chosen arbitrarily, but different values of the enthalpy of reaction will change the magnitude and sign of the contours' slopes.

As seen visually in Figure S4, both temperature (Θ) and potential (Ψ) can easily cross contours of constant $\log_{10} K$, making them powerful thermodynamic tools. Pressure, however, cannot cross constant K contours as easily, requiring a large change in pressure to alter the conversion (keep in mind that $\Pi \propto \log_{10} P$ so an order of magnitude change in P is necessary to change Π). Simply by looking at the colormaps of Equation S15, one can see that qualitatively potential is a better choice than pressure for improving conversion.

We can better compare these thermodynamic driving forces quantitatively by comparing the derivatives of $\log_{10} K$ with respect to each variable. Taking the partial derivatives of Equation S15, we get:

$$\left(\frac{\partial \log_{10} K}{\partial \Pi} \right)_{\Theta, \Psi} = -1 \quad (\text{S20})$$

$$\left(\frac{\partial \log_{10} K}{\partial \Theta} \right)_{\Pi, \Psi} = \frac{1}{\Theta^2}(1 + \Psi) \quad (\text{S21})$$

$$\left(\frac{\partial \log_{10} K}{\partial \Psi} \right)_{\Theta, \Pi} = -\frac{1}{\Theta} \quad (\text{S22})$$

We can see right away from these derivatives that, given $\Theta < 1$ (generally true for reasonable reaction enthalpies and operating temperatures, Table S4), $\log_{10} K$ will scale more favorably with voltage (Ψ) and temperature (Θ) than with pressure (Π). Additionally, given that $\Pi \propto \log P$, K has a logarithmic relationship with pressure, making it a relatively poorer driving force compared to temperature and voltage. In order to better compare

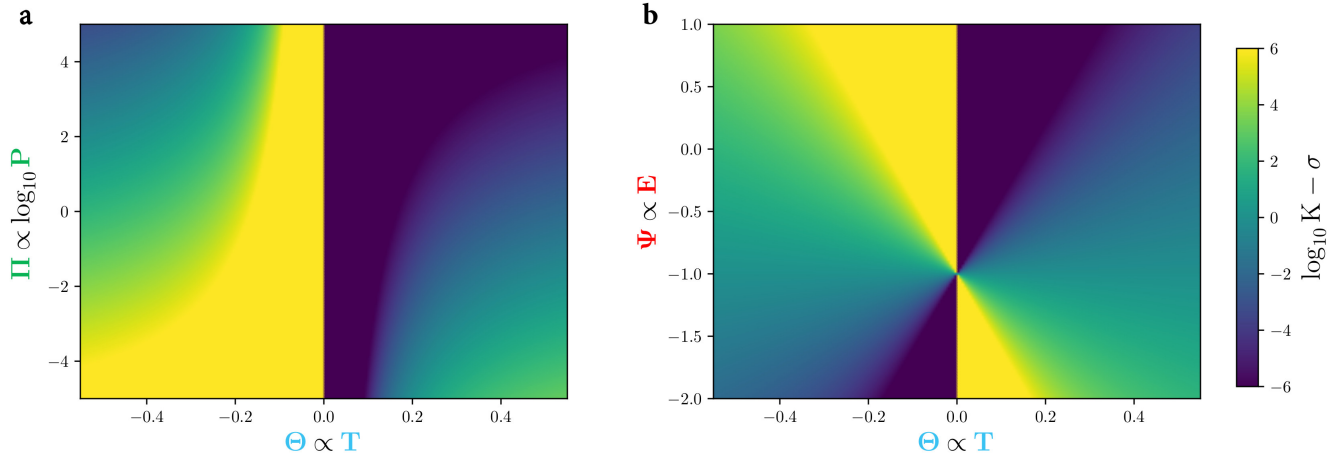


Figure S4: Plots of Equation S15, reproduced from main text. Every reaction can be mapped onto these plots. When no voltage is applied ($\Psi = 0$), the contours of how pressure and temperature affect the equilibrium are visualized (left). At ambient pressure ($\Pi = 0$), the contours of how voltage and temperature affect the equilibrium are visualized (right). Qualitatively, crossing the constant K contours using pressure is more difficult than using voltage or temperature. Note that the colorbar axis is $\log_{10} K - \sigma$ so that the plot remains independent of reaction; different reactions will essentially provide a constant shift from σ that does not change the shape of the plot. Note that crossing $\Theta = 0$ for a given reaction is impossible since the sign of Θ is determined by the reaction enthalpy (a fixed quantity assuming $\Delta C_{P,\text{rxn}} = 0$).

these derivatives, we can compare the derivatives of $\log_{10} K$ with respect to $\log_{10} \Theta$ and $\log_{10} \Psi$. This would put them on equal footing with the derivative with respect to Π so that all the derivatives are with respect to the logarithm of a dimensional thermodynamic parameter. Additionally, this removes some of the arbitrariness of the non-dimensionalization since instead of comparing a "unit" increase in Θ to a "unit" increase in Ψ and Π , we are now comparing *relative* increases in dimensional thermodynamic parameters (e.g., we are comparing the effect of doubling temperature, pressure, and voltage).

$$\left(\frac{\partial \log_{10} K}{\partial \Pi} \right)_{\Theta, \Psi} = -1 \quad (\text{S23})$$

$$\left(\frac{\partial \log_{10} K}{\partial \log_{10} \Theta} \right)_{\Pi, \Psi} = \frac{\log_e 10}{\Theta} (1 + \Psi) \quad (\text{S24})$$

$$\left(\frac{\partial \log_{10} K}{\partial \log_{10} \Psi} \right)_{\Theta, \Pi} = -\frac{\Psi}{\Theta} \log_e 10 \quad (\text{S25})$$

These derivatives further support that qualitatively, crossing voltage and temperature contours is easier and more effective than crossing pressure contours since they have relatively larger derivatives than the derivative with respect to Π . We additionally see that at low values of Ψ , crossing voltage contours may be less effective, but that with moderate to large

values of Ψ (Ψ can easily increase above 2 in some reactions with smaller $|\Delta H_{rxn}^0|$, Table S4), crossing voltage contours becomes significantly more effective than crossing pressure contours. Crossing temperature contours remains perhaps the most effective at increasing K , but temperature is limited in that we cannot practically go to operating temperatures above ca. 1500 K, which is insufficient to drive some reactions.

We have so far stated as fact that $\Theta < 1$ for many reactions, and to back this up, I have provided values for Θ^{ambient} for ammonia synthesis and water splitting:



Table S4: Reaction parameters for ammonia synthesis and water splitting

Rxn	ΔH_{rxn}^0 (kJ/mol)	ΔS_{rxn}^0 (J/mol.K)	$\sum_{i=\text{gas}} \nu_i$	n	Θ^{ambient}	E at $\Psi = 1$
Eq. R1	-46	-99	-1	3	-0.12	-0.16 V
Eq. R2	242	44	0.5	2	0.024	1.25 V

We can see that for these very different reactions, Θ^{ambient} and Ψ have values as we have described above.

S5 Derivation of work and energy exchange

We want to convert our chemical reaction system away from the variables T , P , and E , which are not directly comparable, to quantities that are directly comparable. In particular, we want to compare relevant work and energy quantities for our system, specifically mechanical work input ($\dot{W}_{M,\text{on}}$), heat input (\dot{Q}_{on}) and electrochemical work input ($\dot{W}_{E,\text{on}}$). All of these parameters have units of Watts, and we will **assume continuous, steady state operation of our system with each step being reversible**. Additionally, we will continue to assume that all of our mixtures are **ideal mixtures of ideal gases**. As we all know from thermodynamics, work and heat flow are path variables and should depend on exactly how we operate our system. However, if we constrain our system to operate with **one heat bath** (e.g., the atmosphere), then all reversible paths will result in the same work and heat flux. We have introduced one additional parameter to our system, T^{bath} , but in return work and heat flux become state functions.

The system we will work with is shown in Figure S5, a variation on a Van't Hoff Equilibrium box^{5;6}. In particular, we will first change our system from ambient conditions to reaction conditions, operate the reaction for some extent of reaction at constant T, P, and E, and then return our system to ambient conditions.

We will treat each sub-unit of Figure S5 in turn. First, let's look at the unit that changes the T and P to operating conditions. We can do an entropy (Second law) balance over this

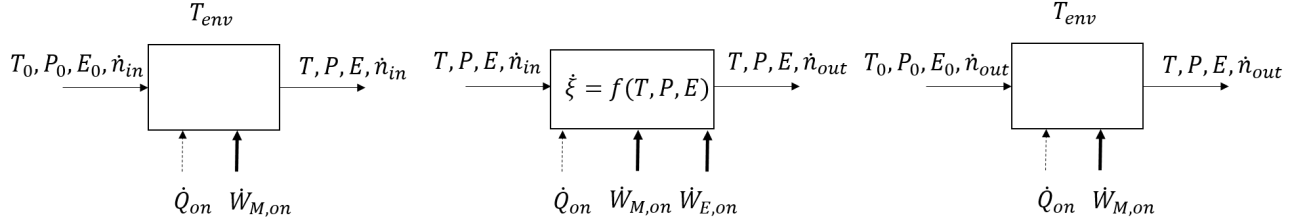


Figure S5: Model for calculating work and heat flow for our system. Each box is a separate unit we will analyze as described in the text. Note that as written, \dot{n}_{in} and \dot{n}_{out} are vectors of mole flowrates with $\dot{n}_{out} = \dot{n}_{in} - \xi\nu$ (ξ is the extent of reaction between 0 and 1 and ν is a vector of the stoichiometric coefficients)

unit and get the following equation for the heat flow.

$$\dot{S}_{universe} = \dot{S}_{unit} + \dot{S}_{environment} - \dot{n}_{in}\bar{S}(T_0, P_0, E_0) + \dot{n}_{in}\bar{S}(T, P, E) \quad (S26)$$

$$0 = -\frac{\dot{Q}_{on}}{T_{bath}} + \dot{n}_{in} \left(C_{P,rxts} \log \frac{T}{T_0} - R \log \frac{P}{P_0} \right) \quad (S27)$$

$$\boxed{\dot{Q}_{on} = \dot{n}_{in}T^{bath} \left(C_{P,rxts} \log \frac{T}{T_0} - R \log \frac{P}{P_0} \right)} \quad (S28)$$

We have assumed steady state ($\dot{S}_{unit} = 0$) and reversible ($\dot{S}_{universe} = 0$), and have used the entropy for an ideal gas. Additionally, R is the ideal gas constant and $C_{P,rxts}$ is the molar average C_P of the reactant mixture. We can next perform an energy (First Law) balance to get the mechanical work on the system.

$$\dot{U} = \dot{Q}_{on} + \dot{W}_{M,on} + \dot{n}_{in}\bar{H}(T_0, P_0, E_0) - \dot{n}_{in}\bar{H}(T, P, E) \quad (S29)$$

$$0 = \dot{Q}_{on} + \dot{W}_{M,on} + \dot{n}_{in}C_{P,rxts}(T_0 - T) \quad (S30)$$

$$\boxed{\dot{W}_{M,on} = \dot{n}_{in}C_{P,rxts}(T - T_0) - \dot{n}_{in}T^{bath} \left(C_{P,rxts} \log \frac{T}{T_0} - R \log \frac{P}{P_0} \right)} \quad (S31)$$

Again, we have assumed steady state and an ideal gas with the enthalpy being only a function of temperature. A few important items to note about these equations: First, we need to specify T^{bath} . We chose this additional parameter instead of a specific thermodynamic path to increase generality of our analysis. In practice, though, our derivation is not so different from an adiabatic compressor followed by a heat exchanger. Second, because our path is reversible, the work and heat flow on the unit after the reactor will essentially be the same expression except with \dot{n}_{out} instead of \dot{n}_{in} and $C_{P,prds}$ instead of $C_{P,rxts}$. Third, because our system is reversible, the work we calculate is the maximum possible work by our system (or the minimum work on our system).

The remaining unit we need to analyze is the reaction unit itself (the post-reactor unit is identical to the pre-reactor unit with some sign changes). We will follow the same procedure as above. Since our reaction is at constant T and P, the environment must also be at T and P for the sake of thermodynamic consistency in our derivation. First, a second law balance gives:

$$\dot{Q}_{\text{on}} = \dot{\xi}T \left(\Delta S_{\text{rxn}}^0 + \Delta C_{P,\text{rxn}} \log \frac{T}{T^0} - \Delta n_{\text{rxn}} R \log \frac{P}{P^0} \right) \quad (\text{S32})$$

$$= \dot{\xi}T \Delta S_{\text{rxn}} \quad (\text{S33})$$

A first law energy balance gives:

$$\dot{W}_{M,\text{on}} + \dot{W}_{E,\text{on}} = -\dot{\xi}T \left(\Delta S_{\text{rxn}}^0 + \Delta C_{P,\text{rxn}} \log \frac{T}{T^0} - \Delta n_{\text{rxn}} R \log \frac{P}{P^0} \right) + \dot{\xi} (\Delta H_{\text{rxn}}^0 + \Delta C_{P,\text{rxn}}(T - T^0)) \quad (\text{S34})$$

$$= \dot{\xi} \Delta G_{\text{rxn}}(T, P) \quad (\text{S35})$$

This makes intuitive sense, but does not allow for the case where the reaction does not allow for mechanical work and the reaction's mechanical work is dissipated as heat. Incorporating the known electrical work allows us to write the following expressions:

$$\boxed{\dot{W}_{E,\text{on}} = -\dot{\xi}nFE} \quad (\text{S36})$$

$$\boxed{\dot{W}_{M,\text{on}} \leq \dot{\xi}(\Delta G_{\text{rxn}}(T, P) + nFE)} \quad (\text{S37})$$

$$\boxed{\dot{Q}_{\text{on}} = \dot{\xi} (\Delta H_{\text{rxn}}^0 + \Delta C_{P,\text{rxn}}(T - T^0)) - (\dot{W}_{M,\text{on}} + \dot{W}_{E,\text{on}})} \quad (\text{S38})$$

Combining Equations S36, S37, and S38 along with Equations S28 and S31 for the pre and post change in state give us an expression for the total work and heat flow of the entire system.

$$\dot{W}_{E,\text{on}} = \eta^{rxn,WE} \dot{W}_{E,\text{on}}^{\text{rxn}} \quad (\text{S39})$$

$$\dot{W}_{M,\text{on}} = \eta^{pre,W} \dot{W}_{M,\text{on}}^{\text{pre}} + \eta^{rxn,W} \dot{W}_{M,\text{on}}^{\text{rxn}} + \eta^{post,W} \dot{W}_{M,\text{on}}^{\text{post}} \quad (\text{S40})$$

$$\dot{Q}_{\text{on}} = \eta^{pre,Q} \dot{Q}_{\text{on}}^{\text{pre}} + \eta^{rxn,Q} \dot{Q}_{\text{on}}^{\text{rxn}} + \eta^{post,Q} \dot{Q}_{\text{on}}^{\text{post}} \quad (\text{S41})$$

Here all of the η^i represent efficiencies that can be put in if more information is known about a system (e.g., if you will not be using an expander to retrieve work $\eta^{post,W} = 0$). For the sake of analysis, we will assume that all $\eta^i = 1$, representing the theoretical minimum work performed on our system and its corresponding heat flow. We then get the following expression for the total work and heat flow in our system given a certain T and P (remember that the extent of reaction is also just a function of T and P). In this derivation we **assume that mechanical work can be exchanged with the reactor**.

$$\dot{W}_{M,on} = (\dot{n}_{in} C_{P,rxts} - \dot{n}_{out} C_{P,prds})(T - T_0) \quad (S42)$$

$$- T^{bath} \left((\dot{n}_{in} C_{P,rxts} - \dot{n}_{out} C_{P,prds}) \log \frac{T}{T_0} - (\dot{n}_{in} - \dot{n}_{out}) R \log \frac{P}{P_0} \right) \quad (S43)$$

$$+ \dot{\xi}(\Delta G_{rxn}(T, P) + nFE) \quad (S44)$$

$$= -\dot{\xi} \Delta C_{P,rxn}(T - T_0) + \dot{\xi} T^{bath} \left(\Delta C_{P,rxn} \log \frac{T}{T_0} - \Delta n_{rxn} R \log \frac{P}{P_0} \right) \quad (S45)$$

$$+ \dot{\xi}(\Delta G_{rxn}(T, P) + nFE) \quad (S46)$$

$$\boxed{\dot{W}_{M,on} = \dot{\xi} \left(\Delta G_{rxn}^0 + (T^{bath} - T) \left[\Delta C_{P,rxn} \log \frac{T}{T_0} - \Delta n_{rxn} R \log \frac{P}{P_0} \right] + nFE \right)} \quad (S47)$$

$$\dot{Q}_{on} = T^{bath} \left((\dot{n}_{in} C_{P,rxts} - \dot{n}_{out} C_{P,prds}) \log \frac{T}{T_0} - (\dot{n}_{in} - \dot{n}_{out}) R \log \frac{P}{P_0} \right) \quad (S48)$$

$$+ \dot{\xi} (\Delta H_{rxn}^0 + \Delta C_{P,rxn}(T - T^0) - \Delta G_{rxn}(T, P)) \quad (S49)$$

$$= -\dot{\xi} T^{bath} \left(\Delta C_{P,rxn} \log \frac{T}{T_0} - \Delta n_{rxn} R \log \frac{P}{P_0} \right) \quad (S50)$$

$$+ \dot{\xi} (\Delta H_{rxn}^0 + \Delta C_{P,rxn}(T - T^0) - \Delta G_{rxn}(T, P)) \quad (S51)$$

$$\boxed{\dot{Q}_{on} = \dot{\xi} \left(T \Delta S_{rxn}^0 - (T^{bath} - T) \left[\Delta C_{P,rxn} \log \frac{T}{T_0} - \Delta n_{rxn} R \log \frac{P}{P_0} \right] \right)} \quad (S52)$$

$$\boxed{\dot{W}_{E,on} = -\dot{\xi} nFE} \quad (S53)$$

If we **assume that no mechanical work can be exchanged with the reactor** (a reasonable industrial situation that corresponds to us relaxing the constraint $\dot{S}_{universe} = 0$ for the reactor unit itself), we get the following:

$$\boxed{\dot{W}_{E,on} = -\dot{\xi} nFE} \quad (S54)$$

$$\boxed{\dot{W}_{M,on} = \dot{\xi} \left(-\Delta C_{P,rxn}(T - T_0) + T^{bath} \left[\Delta C_{P,rxn} \log \frac{T}{T_0} - \Delta n_{rxn} R \log \frac{P}{P_0} \right] \right)} \quad (S55)$$

$$\boxed{\dot{Q}_{on} = \dot{\xi} \left(-T^{bath} \left[\Delta C_{P,rxn} \log \frac{T}{T_0} - \Delta n_{rxn} R \log \frac{P}{P_0} \right] + \Delta H_{rxn}^0 + \Delta C_{P,rxn}(T - T_0) + nFE \right)} \quad (S56)$$

Interestingly enough, even though we began this analysis allowing enthalpy to vary with temperature, we find that in these final expressions for work and heat flow that the enthalpic terms all contain $\Delta C_{P,rxn}$. We previously assumed this value to be zero, and while this is not a good assumption for quantitative results, **it is a reasonable assumption to qualitatively study the system**. From here forward, we will assume that **no mechanical work is exchanged between the reactor and the environment**. With these assumptions, we get the following expressions for work and heat flows:

$$\dot{W}_{E,on} = -\dot{\xi}nFE \quad (\text{S57})$$

$$\dot{W}_{M,on} = -\dot{\xi}\Delta n_{\text{rxn}}RT^{\text{bath}} \log \frac{P}{P_0} \quad (\text{S58})$$

$$\dot{Q}_{\text{on}} = \dot{\xi} \left(\Delta n_{\text{rxn}}RT^{\text{bath}} \log \frac{P}{P_0} + \Delta H_{\text{rxn}}^0 + nFE \right) \quad (\text{S59})$$

These are remarkably simple expressions that still make qualitative sense. The electrical work depends on the voltage and conversion by definition. The mechanical work depends on the conversion and the pressure, with any temperature terms having been neglected at this point in the simplification. The heat flow is a function of the reaction enthalpy, the pressure, and the potential as well as conversion. We note that temperature does not appear explicitly in these expressions due to the fact that the temperature components cancel out to enough of a degree that we neglect them with our assumption that the enthalpy of reaction is independent of temperature. However, these expressions still depend strongly on temperature since the conversion will depend strongly on temperature.

A major assumption that we are making is that the heat bath used to bring the reactants to operating conditions and the heat bath used to bring the products to ambient conditions is at the same T^{bath} . This is likely a poor assumption in practice, but for the sake of qualitative analysis it is sufficient to give us an idea of the functional form of the work and heat flux terms in terms of simple parameters while avoiding complications from the various heat capacities of reactants and products.

As it turns out, we can write our equations for work and heat flow in non-dimensional form as in the main text. Let us define new non-dimensional quantities:

$$\Omega_{W,E} = \frac{\dot{W}_{E,on}}{\Delta H_{\text{rxn}}^0} \quad (\text{S60})$$

$$\Omega_{W,M} = \frac{\dot{W}_{M,on}}{\Delta H_{\text{rxn}}^0} \quad (\text{S61})$$

$$\Omega_Q = \frac{\dot{W}_{\text{on}}}{\Delta H_{\text{rxn}}^0} \quad (\text{S62})$$

Additionally, note that $\dot{\xi} = z(\log_{10} K_{\text{eq}}) = z(f(\Theta, \Psi, \Pi) + \sigma)$, where $f = -1/\Theta - \Psi/\Theta - \Pi$. The exact function form of $\dot{\xi}$ depends on the reaction, but we know it is roughly logistic in shape and spans 0 to 1 from $\log_{10} K_{\text{eq}} = -5$ to $\log_{10} K_{\text{eq}} = 5$, respectively.

We can now write:

$$\Omega_{W,E} = -z(f(\Theta, \Psi, \Pi) + \sigma)\Psi \quad (\text{S63})$$

$$\Omega_{W,M} = -z(f(\Theta, \Psi, \Pi) + \sigma)\Theta^{\text{bath}}\Pi \quad (\text{S64})$$

$$\Omega_Q = z(f(\Theta, \Psi, \Pi) + \sigma)(\Theta^{\text{bath}}\Pi + \Psi + 1) \quad (\text{S65})$$

Our equations for work and heat are easily nondimensionalized with our nondimensional groups from the discussion on chemical equilibrium. Note that as expected, energy for the

entire process is conserved:

$$\sum_i \Omega_i = z(f(\Theta, \Psi, \Pi) + \sigma) \quad (\text{S66})$$

What we get from Equation S66, is intuitive: all of the energy exchange with our system must add up to the conversion times the enthalpy of reaction (this is just conservation of energy). Note that this equivalence of energy

S6 Redefinition of axes to collapse K contours

We would like to compare many reactions to each other on the same set of axes. This requires a set of axes on which the equilibrium contours are the same for every reaction. Specifically, we need our contours (z -levels) to be $\log_{10} K$ instead of $\log_{10} K - \sigma$. If we look back at Equation (S15), we see that incorporating σ into our x -axis or y -axis is nontrivial. In fact, there are a few different ways we could redefine the axes.

Perhaps the simplest redefinition would be to keep the axes as close as possible to the original non-dimensional variables. Accordingly, we can set $x = \Theta$ and $y = \Pi - \sigma$ for the pressure-temperature case, meaning that $\log_{10} K = -1/x - y$. Similarly, for the voltage-temperature case, we would have $x = \Theta$ and $y = \Psi - \sigma\Theta$, meaning that $\log_{10} K = -1/x - y/x$. This formulation could work, but we are stuck with two plots with different equations for equilibrium contours, making interpretation difficult. If we wanted to combine the influence of voltage and pressure onto one axis so that we can describe reactions on a single plot, we could define $x = \Theta$ and $y = \Psi/\Theta + \Pi - \sigma$, meaning that $\log_{10} K = -1/x - y$. While this method results in a single plot for comparing pressure, voltage, and temperature, it does not facilitate easy comparison of reactions. Intuitively, reactions with larger enthalpies (ΔH_{rxn}^0) will have smaller values of Θ^{ambient} since $\Theta \propto 1/\Delta H_{\text{rxn}}^0$, but comparing reactions quantitatively by inspection is difficult. Instead, it would be extremely useful if we could represent a reaction by a single point, $(x, y)_{\text{rxn}}^{\text{ambient}}$, such that the point itself was informative about the reaction relative to equilibrium contours and such that we would “add” reaction points $(x_1, y_1)_{\text{rxn},1}^{\text{ambient}}$ and $(x_2, y_2)_{\text{rxn},2}^{\text{ambient}}$ to generate a new reaction point $(x_1 + x_2, y_1 + y_2)_{\text{rxn}}^{\text{ambient}}$ that represents adding the two reaction chemical equations as well (this is discussed further in the main text). Accordingly, we need to define $x = 1/\Theta$ and $y = \Psi/\Theta + \Pi - \sigma$, meaning $\log_{10} K = -x - y$. This means that constant contours on this axis will be of the form $y = -x - \log_{10} K$. As an additional benefit, these parallel lines are easier to visualize and compare to reaction points than the contours would be if we had defined $x = \Theta$ (those contours being represented by $y = -1/x - \log_{10} K$).

There are a few points to note on these new axes. As noted in the main text, each reaction is given by the point:

$$(x, y)_{\text{rxn}}^{\text{ambient}} = \left(\frac{1}{\Theta^{\text{ambient}}}, -\sigma \right) = \left(\frac{\Delta H_{\text{rxn}}^0}{RT^0 \log 10}, -\frac{\Delta S_{\text{rxn}}^0}{R \log 10} \right) \quad (\text{S67})$$

The equilibrium potential for a given reaction is defined by the potential when $\log_{10} K = 0$, or when $y = -x$ in these coordinates. At ambient conditions, we know that $\Psi^{\text{eq}}/\Theta^{\text{ambient}} -$

$\sigma = y^{\text{eq}} = -x^{\text{ambient}}$. From this, we can get:

$$\Psi^{\text{eq}} = \Theta^{\text{ambient}}(y^{\text{eq}} + \sigma) \quad (\text{S68})$$

$$= \Theta^{\text{ambient}}(y^{\text{eq}} - y^{\text{ambient}}) \quad (\text{S69})$$

$$= (y^{\text{eq}} - y^{\text{ambient}})/x^{\text{ambient}} \quad (\text{S70})$$

$$= -(y^{\text{eq}} - y^{\text{ambient}})/y^{\text{eq}} \quad (\text{S71})$$

$$= -1 + \frac{y^{\text{ambient}}}{y^{\text{eq}}} \quad (\text{S72})$$

$$\Psi^{\text{eq}} = -1 - \frac{y^{\text{ambient}}}{x^{\text{ambient}}} \quad (\text{S73})$$

We can see that the *non-dimensional* equilibrium potential is proportional to the ratio of y^{ambient} to y^{eq} , or equivalently the ratio y^{ambient} to x^{ambient} which is the slope of a line from $(0, 0)$ to $(x, y)_{\text{rxn}}^{\text{ambient}}$, a simple and intuitive read from the plot. However, there is an even simpler measure of equilibrium potential available from this plot that makes these axes extremely powerful and is described in detail in Discussion S7.

In these redefined axes, a change in voltage or pressure will result in a vertical movement on the axes, and an increase (decrease) in temperature corresponds to a movement toward (away from) the point $(0, \Pi - \sigma)$ (movement along the line given by $y = -\sigma + \Pi + \Psi x$). A reproduction of the comparison of multiple reactions from the text if provided with the addition of vertical lines representing an increase in pressure by an order of magnitude (Figure S6).

S7 Scaling of reaction stoichiometry to compare reactions

In order to make a proper comparison between reactions, we need to normalize the stoichiometry. To do this, each reaction is scaled to a fixed number of electrons transferred in the reaction (fixed n_{e^-}). This means that each of ΔH_{rxn} , ΔS_{rxn} , and Δn_{rxn} are rescaled such that $n_{e^-} = \rho$. The big question is: what value of ρ should be used? A value between 1 and 4 makes the most sense as it leads to reactions collapsing visually on these axes such that the reactions can be compared easily while still being spaced sufficiently apart. To aid with readability, it makes sense to scale to a number that will result in a meaningful point (x, y) . We have therefore chosen to scale to $n_{e^-} = 2.956$. This value, although it appears arbitrary, is actually chosen such that a reaction at point (x, y) will have a *dimensional* equilibrium potential $E^{\text{eq}} = -20(x + y)$ (E^{eq} in mV).

We can see that for a reaction defined by,

$$(x, y)_{\text{rxn}}^{\text{ambient}} = \left(\frac{1}{\Theta^{\text{RT}}}, -\sigma \right) = \left(\frac{\Delta H_{\text{rxn}}^0}{RT^0 \log 10}, -\frac{\Delta S_{\text{rxn}}^0}{R \log 10} \right) \quad (\text{S74})$$

the sum of the coordinates is

- ◆ $1/2\text{N}_2 + 3/2\text{H}_2 \rightarrow \text{NH}_3$
- ▼ $\text{NH}_3 \rightarrow 1/2\text{N}_2 + 3/2\text{H}_2$
- ▲ $\text{H}_2 + \text{CO} + \text{C}_2\text{H}_4 \rightarrow \text{C}_3\text{H}_6\text{O}$
- ★ $\text{C}_3\text{H}_8 \rightarrow \text{C}_3\text{H}_6 + \text{H}_2$
- $2\text{H}_2\text{S} + \text{O}_2 \rightarrow 2\text{S}(\ell) + 2\text{H}_2\text{O}$
- ◆ $6\text{CH}_4 \rightarrow \text{C}_6\text{H}_6 + 9\text{H}_2$
- $\text{CO}_2 + 3\text{H}_2 \rightarrow \text{CH}_3\text{OH} + \text{H}_2\text{O}$
- $\text{CO} + 2\text{H}_2 \rightarrow \text{CH}_3\text{OH}$
- ▼ $\text{CO}_2 + \text{CH}_4 \rightarrow 2\text{H}_2 + 2\text{CO}$
- ◆ $\text{H}_2\text{O} \rightarrow \text{H}_2 + 1/2\text{O}_2$
- $\text{CO}_2 \rightarrow \text{CO} + 1/2\text{O}_2$
- $\text{N}_2 + 3\text{H}_2\text{O} \rightarrow 2\text{NH}_3 + 3/2\text{O}_2$
- ◀ $2\text{CO}_2 + 2\text{H}_2\text{O} \rightarrow \text{C}_2\text{H}_4 + 3\text{O}_2$
- ▶ $\text{C}_2\text{H}_4 + \text{H}_2\text{O} \rightarrow \text{C}_2\text{H}_4\text{O} + \text{H}_2$
- ▲ $2\text{NaCl(s)} + 2\text{H}_2\text{O}(\ell) \rightarrow \text{H}_2 + \text{Cl}_2 + 2\text{NaOH(s)}$
- ▼ $2\text{Al}_2\text{O}_3(\text{s}) + 3\text{C(s)} \rightarrow 4\text{Al(s)} + 3\text{CO}_2$
- ◆ $2\text{C}_3\text{H}_3\text{N} + \text{H}_2\text{O} \rightarrow \text{C}_6\text{H}_8\text{N}_2 + 1/2\text{O}_2$

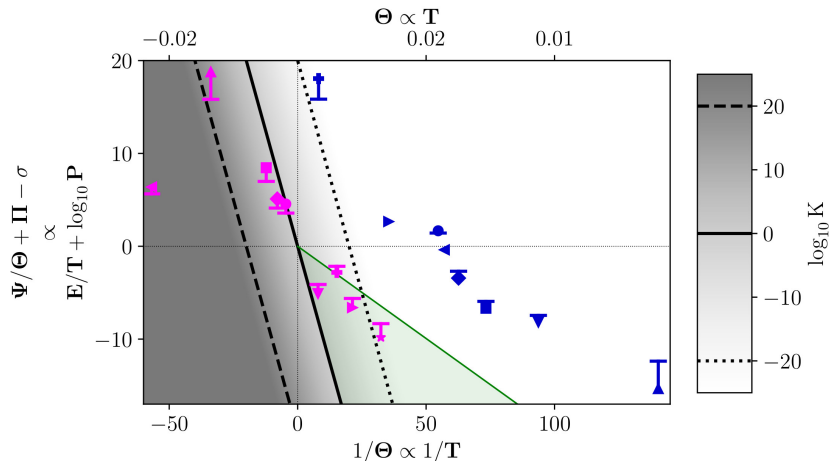


Figure S6: Reproduction from main text of comparison of multiple reactions on the same axes. Each point represents a chemical reaction, with color denoting whether the reaction is typically conducted thermochemically (pink) or electrochemically (blue). Each reaction point is such that $(x, y)^{\text{ambient}} \propto (\Delta H_{\text{rxn}}^0, -\Delta S_{\text{rxn}}^0)$ and can be interpreted as described in Figure S7. Vertical lines represent an increase in pressure by one order of magnitude. The green shading indicates the area where an elevated temperature of less than ~ 1500 K can reach $K = 1$, and a quantitative visual divide based on reaction enthalpies and entropies distinguishes between reactions driven with electrochemistry versus those driven with thermochemistry. Note that the stoichiometry depicted in the legend is for readability; all reactions have been scaled to have the same number of electrons for best comparison (Supplemental Derivation S7). To be consistent, chemical formulas were used for all species in the legend, but the following formulas are not unique and refer to the specified chemical: $\text{C}_3\text{H}_6\text{O}$ (propanal), $\text{C}_2\text{H}_4\text{O}$ (ethylene oxide), C_3H_6 (propene), C_6H_6 (benzene), $\text{C}_3\text{H}_3\text{N}$ (acrylonitrile), and $\text{C}_6\text{H}_8\text{N}_2$ (adiponitrile). Raw thermodynamic data given in Tables S1 and S2.^{1;2;3;4}.

$$(x + y) = \frac{\Delta H_{\text{rxn}}^0}{RT^0 \log 10} - \frac{\Delta S_{\text{rxn}}^0}{R \log 10} \quad (\text{S75})$$

$$= \frac{\Delta G_{\text{rxn}}^0}{RT^0 \log 10} \quad (\text{S76})$$

$$= \frac{-n_e F}{RT^0 \log 10} E^{\text{eq}} \quad (\text{S77})$$

Solving for n_e such that $\frac{-nF}{RT^0 \log 10} = -0.05 \text{ mV}^{-1}$ (arbitrarily chosen so that the points will be well spaced on the plot and the numbers will be easy for mental math) gives $n_e = 2.956$. Unlike previously where we equated the *non-dimensional* equilibrium potential with a ratio of y^{ambient} to x^{ambient} , here we see that the *dimensional* equilibrium potential can be read directly from this plot. As a corollary to this fact, we can see that reaction points that have $|E^{\text{eq}}| \leq 1 \text{ V}$ must satisfy the condition that $1000 \text{ mV} \geq | -20(x + y)|$, or equivalently must satisfy $-50 - x \leq y \leq 50 - x$. Although we have not drawn these lines, they unsurprisingly show that voltages of order 1 V are sufficient to drive thermodynamic conversion of most chemical reactions encountered in the wild.

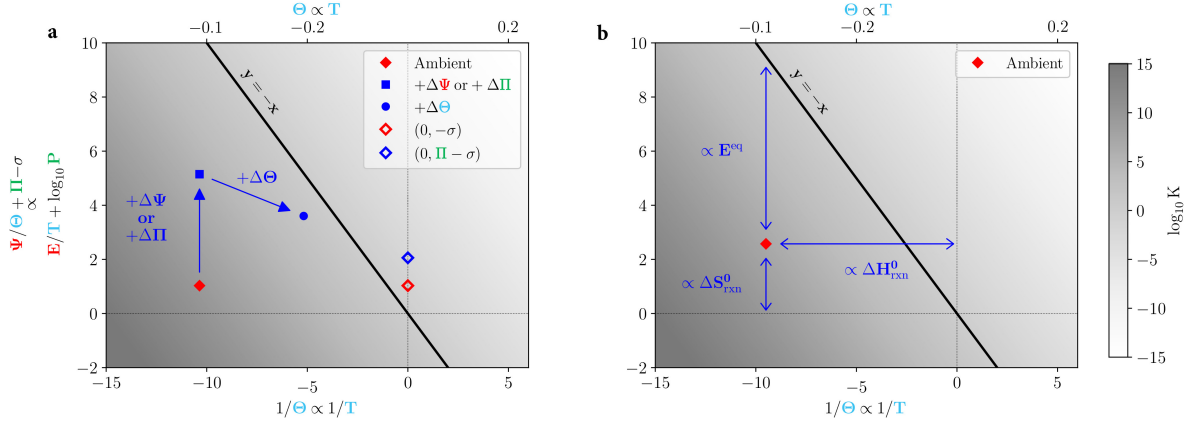


Figure S7: Reproduction from main text. Redefined axes such that all reactions have the same equilibrium K contours. A contour corresponding to $K = 1$ is indicated with a diagonal black line. The filled red diamonds represent an example reaction point at ambient conditions given by Equation (S67). An increase in either pressure (Π) or voltage (Ψ) is a vertical movement on these axes (A, new reaction point given by blue square) and an increase in temperature (Θ) is a movement towards the point $(0, \Pi - \sigma)$ (A, new reaction point given by blue circle, movement along the line connecting to the empty blue diamond). As shown, the distance from the reaction point to the y -axis is proportional to ΔH_{rxn}^0 , the distance to the x -axis is proportional to ΔS_{rxn}^0 , and the distance to the solid black line ($y = -x$) is proportional to the *dimensional* equilibrium potential of the reaction (B). Further details in Supplemental Derivations S5 and S6

S8 Quantitative limits on thermochemical and electrochemical reactions

In the main text, we have chosen ~ 1500 K as an upper limit for practical temperatures for thermochemical processes in the chemical industry. This value was chosen to represent a reasonable upper limit that encompasses the vast majority of chemical processes found in the chemical industry⁷. However, there are some processes that use temperatures greater than 1500 K (e.g., flue dust gasification, industrially known as the Koppers-Totzek process). Changing the upper limit of temperature only affects the slope of the shaded area in Figure 6 from the main text; e.g., using 2000 K or for an upper limit only extends the shaded region marginally (Figure S8). In this work, the limit of 1500 K is not meant to be a hard limit dividing what is possible and not possible for temperature to drive a chemical reaction. Instead, 1500 K is meant to provide a reasonable guide and ground the analysis with real temperatures; if a chemical reaction is just outside of the shaded region, this does not imply it cannot be driven with temperature, only that the temperature necessary would be large and needs to be taken into consideration when designing a process.

It is important to note that for the sake of generality, we have used the equilibrium constant exclusively as a metric for determining whether a reaction can be driven at a certain set of operating conditions. In practice, it is possible to drive reactions at conditions that would appear untenable from a simple thermodynamic plot through engineering ingenuity and system design. For example, by removing one of the products, one can leverage Le

- ◆ $1/2\text{N}_2 + 3/2\text{H}_2 \rightarrow \text{NH}_3$
- ▼ $\text{NH}_3 \rightarrow 1/2\text{N}_2 + 3/2\text{H}_2$
- ▲ $\text{H}_2 + \text{CO} + \text{C}_2\text{H}_4 \rightarrow \text{C}_3\text{H}_6\text{O}$
- ★ $\text{C}_3\text{H}_8 \rightarrow \text{C}_3\text{H}_6 + \text{H}_2$
- $2\text{H}_2\text{S} + \text{O}_2 \rightarrow 2\text{S}(\ell) + 2\text{H}_2\text{O}$
- ◆ $6\text{CH}_4 \rightarrow \text{C}_6\text{H}_6 + 9\text{H}_2$
- $\text{CO}_2 + 3\text{H}_2 \rightarrow \text{CH}_3\text{OH} + \text{H}_2\text{O}$
- $\text{CO} + 2\text{H}_2 \rightarrow \text{CH}_3\text{OH}$
- ▼ $\text{CO}_2 + \text{CH}_4 \rightarrow 2\text{H}_2 + 2\text{CO}$
- ◆ $\text{H}_2\text{O} \rightarrow \text{H}_2 + 1/2\text{O}_2$
- $\text{CO}_2 \rightarrow \text{CO} + 1/2\text{O}_2$
- $\text{N}_2 + 3\text{H}_2\text{O} \rightarrow 2\text{NH}_3 + 3/2\text{O}_2$
- ◀ $2\text{CO}_2 + 2\text{H}_2\text{O} \rightarrow \text{C}_2\text{H}_4 + 3\text{O}_2$
- ▶ $\text{C}_2\text{H}_4 + \text{H}_2\text{O} \rightarrow \text{C}_2\text{H}_4\text{O} + \text{H}_2$
- ▲ $2\text{NaCl(s)} + 2\text{H}_2\text{O}(\ell) \rightarrow \text{H}_2 + \text{Cl}_2 + 2\text{NaOH(s)}$
- ▼ $2\text{Al}_2\text{O}_3(\text{s}) + 3\text{C(s)} \rightarrow 4\text{Al(s)} + 3\text{CO}_2$
- ◆ $2\text{C}_3\text{H}_3\text{N} + \text{H}_2\text{O} \rightarrow \text{C}_6\text{H}_8\text{N}_2 + 1/2\text{O}_2$

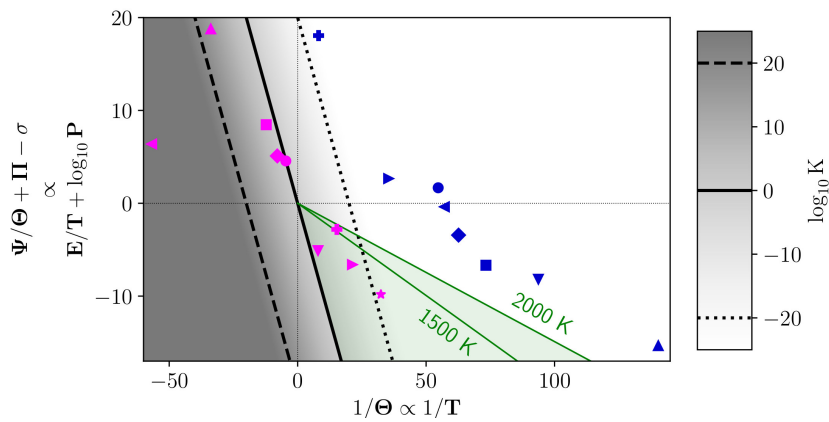


Figure S8: Reproduction from main text of comparison of multiple reactions on the same axes. Extending the green-shaded region extended from 1500 K to 2000 K. Changing the temperature cutoff within a reasonable range of values does not alter our conclusions.

Chatelier's principle to help drive a reaction and push the equilibrium toward a desired product. This is leveraged in solar thermal water splitting and carbon dioxide splitting at temperatures ranging from 1000 K to 1500 K where the oxygen product is incorporated into the metal oxide catalyst in a multi-step process, leading to an equilibrium shift that favors hydrogen or carbon monoxide in the cases of water splitting and carbon dioxide reduction, respectively^{8,9}. Other common uses for this technique include the removal of water to enable dehydration reactions, and reactive distillation systems. Despite this, in general the equilibrium constant represents a very good proxy for thermodynamic feasibility with the caveat that careful system engineering can help drive reactions when thermodynamic operating conditions indicate a reaction is infeasible.

S9 Simple Descriptors

Some of the major points about reaction feasibility and thermodynamic equilibrium can be determined from simple descriptors without the need for our non-dimensionalization scheme. For example, simply looking at the sign of ΔG_{rxn} at a given temperature will tell us whether the reaction is thermodynamically favorable, and $T_{\text{char}} = \Delta H_{\text{rxn}}^0 / \Delta S_{\text{rxn}}^0$ provides us with a metric of whether temperature alone can drive a given reaction to thermodynamic equilibrium. Other potential descriptors such as $\sum_i \nu_i$ for a reaction tell us the influence of pressure and $E_{\text{eq}} = \Delta G_{\text{rxn}} / nF$ gives an idea of how much voltage is necessary to drive the reaction. Individually, each of these descriptors is extremely useful, but they unfortunately must be calculated for each specific reaction, often at various operating conditions. These descriptors are therefore useful, but do not contain the same amount of information as our visualization in Figure S6. As an example, using ΔG_{rxn} and T_{char} as descriptors, we have plotted the same data as in Figure S6 on new axes (Figure S9). While discrimination via these quantities can tell us whether a reaction is capable of being driven by temperature to equilibrium conversion, they do not provide information about the magnitude of the influence of temperature, pressure, and voltage, and they do not provide any information on the

influence of pressure on the reaction. When temperature, pressure, and voltage deviate from ambient conditions, the new equilibrium conversion is readily apparent on Figure S6 as the axes scale with these thermodynamic quantities as discussed in the main text. Additionally, the influence of pressure on a reaction can be quickly ascertained on our axes based on the y-value of the point (or explicitly shown in Figure S6 with the vertical lines), whereas the role of pressure is difficult to determine from the Gibbs free energy of reaction or the equilibrium temperature. Because our axes allow for quantification of the influence of thermodynamic parameters on the equilibrium conversion, our axes can be used to investigate such questions as: what is the equilibrium conversion of ammonia synthesis at operating conditions? And: which reactions can rely on pressure to increase equilibrium conversion at conditions which facilitate fast kinetics? The answers to these questions are not novel—we could easily gather additional descriptors similar to those mentioned above that would encompass more aspects of the system. However, with our carefully chosen non-dimensional scheme, we can visualize all of these descriptors on a single plot for multiple reactions instead of requiring a list of descriptors for each individual reaction at every temperature, pressure, and voltage of interest. We can also add and subtract reactions on our proposed axes for simple exploration of possible reactants and products as discussed in the main text.

- ◆ $1/2\text{N}_2 + 3/2\text{H}_2 \rightarrow \text{NH}_3$
- ▼ $\text{NH}_3 \rightarrow 1/2\text{N}_2 + 3/2\text{H}_2$
- ▲ $\text{H}_2 + \text{CO} + \text{C}_2\text{H}_4 \rightarrow \text{C}_3\text{H}_6\text{O}$
- ★ $\text{C}_3\text{H}_8 \rightarrow \text{C}_3\text{H}_6 + \text{H}_2$
- ◀ $2\text{H}_2\text{S} + \text{O}_2 \rightarrow 2\text{S}(\ell) + 2\text{H}_2\text{O}$
- ✚ $6\text{CH}_4 \rightarrow \text{C}_6\text{H}_6 + 9\text{H}_2$
- $\text{CO}_2 + 3\text{H}_2 \rightarrow \text{CH}_3\text{OH} + \text{H}_2\text{O}$
- $\text{CO} + 2\text{H}_2 \rightarrow \text{CH}_3\text{OH}$
- ▶ $\text{CO}_2 + \text{CH}_4 \rightarrow 2\text{H}_2 + 2\text{CO}$
- ◆ $\text{H}_2\text{O} \rightarrow \text{H}_2 + 1/2\text{O}_2$
- $\text{CO}_2 \rightarrow \text{CO} + 1/2\text{O}_2$
- $\text{N}_2 + 3\text{H}_2\text{O} \rightarrow 2\text{NH}_3 + 3/2\text{O}_2$
- ◀ $2\text{CO}_2 + 2\text{H}_2\text{O} \rightarrow \text{C}_2\text{H}_4 + 3\text{O}_2$
- ▶ $\text{C}_2\text{H}_4 + \text{H}_2\text{O} \rightarrow \text{C}_2\text{H}_4\text{O} + \text{H}_2$
- ▲ $2\text{NaCl(s)} + 2\text{H}_2\text{O}(\ell) \rightarrow \text{H}_2 + \text{Cl}_2 + 2\text{NaOH(s)}$
- ▼ $2\text{Al}_2\text{O}_3(\text{s}) + 3\text{C(s)} \rightarrow 4\text{Al(s)} + 3\text{CO}_2$
- ✚ $2\text{C}_3\text{H}_3\text{N} + \text{H}_2\text{O} \rightarrow \text{C}_6\text{H}_8\text{N}_2 + 1/2\text{O}_2$

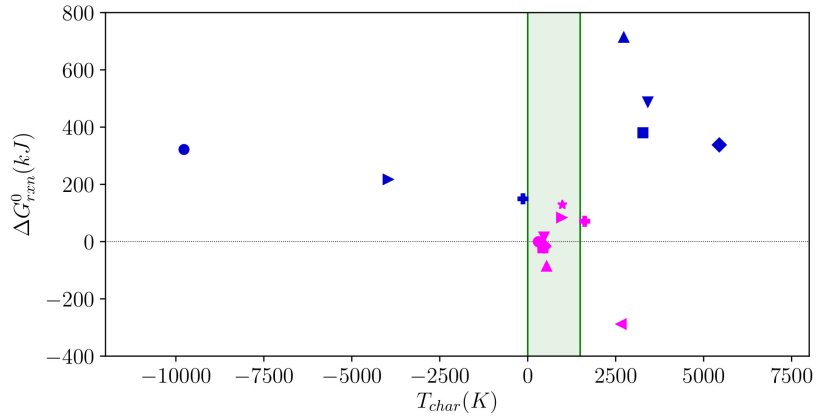


Figure S9: Transformation of Figure S6 data to potential binary descriptors as axes. Although some of the information is preserved on these axes, there is a significant loss of information as described in SI Appendix, Discussion 8.

Supplemental References

References

- [1] Burgess, D. Thermochemical Data. In NIST Chemistry WebBook, NIST Standard Reference Database Number 69, (Linstrom, P. and Mallard, W., eds), chapter Thermochem. National Institute of Standards and Technology Gaithersburg, MD.
- [2] (2020). Dortmund Data Bank.
- [3] Lange, N. A. (1999). Lange's Handbook of Chemistry. 15 edition, McGraw-Hill, Inc.
- [4] Gao, C. W., Allen, J. W., Green, W. H. and West, R. H. (2016). Reaction Mechanism Generator: Automatic construction of chemical kinetic mechanisms. Computer Physics Communications 203, 212–225.
- [5] Bazhin, N. M. (2011). Mechanism of electric energy production in galvanic and concentration cells. Journal of Engineering Thermophysics 20, 302–307.
- [6] Bazhin, N. M. and Parmon, V. N. (2007). Conversion of the chemical reaction energy into useful work in the Van't Hoff equilibrium box. Journal of Chemical Education 84, 1053–1055.
- [7] Weissermel, K. and Arpe, H. (2003). Industrial Organic Chemistry.
- [8] Hao, Y., Yang, C.-K. and Haile, S. M. (2014). Ceria-Zirconia Solid Solutions ($\text{Ce}_{1-x}\text{Zr}_x\text{O}_{2-\delta}$, $x \leq 0.2$) for Solar Thermochemical Water Splitting: A Thermodynamic Study. Chemistry of Materials 26, 6073–6082.
- [9] Furler, P., Scheffe, J., Gorbar, M., Moes, L., Vogt, U. and Steinfeld, A. (2012). Solar Thermochemical CO₂ Splitting Utilizing a Reticulated Porous Ceria Redox System. Energy & Fuels 26, 7051–7059.